Silicon (2022) 14:10535–10558
https://doi.org/10.1007/s12633-022-01786-5

ORIGINAL PAPER

Compressive Strengths and Microstructural Properties of Geopolymeric Materials Arising from the Addition of Semi-crystalline Alumina to Silica-rich Aluminosilicate Sources

Hamed I. Riyap[1] · B. K. Ngongang[1] · Hervé Kouamo Tchakouté[1,2] · C. P. Nanseu-Njiki[1] · C. H. Rüscher[2]

Received: 7 December 2021 / Accepted: 21 February 2022 / Published online: 11 March 2022

Abstract

This work aims to investigate the behaviour of the semi-crystalline alumina added to the aluminosilicates rich in amorphous and crystalline silica during the geopolymerization. Waste fired brick and metakaolin used in this work are rich in amorphous silica and quartz, respectively. Bauxite calcined at 600 °C was used as a semi-crystalline alumina source. The calcined product was added to each aluminosilicate with mass ratios calcined bauxite/metakaolin or calcined bauxite/waste fired brick equals 0, 0.1, 0.2, 0.3 and 0.4. Geopolymer pastes were obtained by adding sodium waterglass to each composition. The hardened pastes were cured at room temperature for 28 days before characterization. The compressive strengths of the geopolymer materials when the mass ratios of calcined bauxite/metakaolin are ranging from 0 to 0.3 increase from 36.33 to 55.09 MPa and drop from 55.09 to 43.19 MPa when that mass ratios increase from 0.3 to 0.4. Whereas those from waste fired brick decrease from 47.81 to 19.91 MPa with increasing the mass ratios. The spectra of the energy dispersive X-ray analysis of geopolymer materials from metakaolin and the one from waste fired brick without addition indicate the formation of Si-rich geopolymer networks. Whereas the one from waste fired brick after the addition of semi-crystalline alumina are mainly composed of Al-rich geopolymer structures. It can be concluded that the semi-crystalline alumina added to the metakaolin spread in the network of the final products while this alumina does not react with amorphous silica contained in the structure of waste fired brick during the geopolymerization.

Keywords Amorphous silica · Quartz · Semi-crystalline alumina · Metakaolin · Waste fired brick · Geopolymer materials

Highlights
- Calcined bauxite was added to metakaolin and waste fired brick using different massratios.
- Each obtained powder was used to prepare geopolymer using sodium waterglass fromrice husk ash.
- The strengths of the geopolymers from metakaolin increase from 36.33 to 55.09 MPawhen the mass ratios increase from 0 to 0.3.
- The strengths drop from 55.09 to 43.19 MPa when that mass ratios decrease from 0.3to 0.4.
- The strengths of geopolymers from waste fired brick from waste fired brick decreasewith increasing that mass ratios.

✉ Hervé Kouamo Tchakouté
htchak@yahoo.fr; hervetchakoute@gmail.com

[1] Laboratory of Analytical Chemistry, Faculty of Science, Department of Inorganic Chemistry, University of Yaounde I, P.O. Box 812, Yaounde, Cameroon

[2] Institut für Mineralogie, Leibniz Universität Hannover, Callinstrasse 3, D-30167 Hannover, Germany

1 Introduction

Geopolymer material which was introduced by Davidovits in 1978 is an inorganic polymer generally obtained at room or slightly elevated temperature [1]. Nevertheless, a synthesis of the literature showed that the temperature of the curing geopolymer material depends on the reactivity of the aluminosilicate source and also on the chemical reagent used. Tchakouté et al. [2] used a semi-adiabatic test to estimate the temperature of the reaction medium after adding sodium waterglass to metakaolin. They reported that the temperature of the reaction medium that entails the formation of geopolymer gel is about 38 °C. So, an exothermic reaction occurs during the synthesis of the geopolymer materials. It is worth noting that this exothermic reaction is different to the curing temperature. The chemical ingredient denoted hardener generally used for the preparation of geopolymer material is sodium waterglass with a molar ratio SiO_2/Na_2O equal to 1.5 [3]. For the past few years, several researchers used

Table 1 Chemical compositions of kaolin (Dib_2), bauxite (BaX), rice husk ash (RHA) and waste fired bricks (WB) in wt%. LOI: Loss on Ignition at 1000 °C for 4 h

Samples Oxides	Dib_2 Melele et al. [26]	BaX (Tchamba et al. [25]	RHA Melele et al. [26]	WB (Beleuk à Moungam et al. [27]
Na_2O	<0.10	/	/	/
MgO	0.10	/	0.28	0.323
Al_2O_3	25.40	58.10	0.58	22.50
SiO_2	59.60	1.00	93.20	60.98
P_2O_5	0.078	0.17	/	0.331
SO_3	<0.02	0.07	/	/
K_2O	0.32	/	3.05	0.932
CaO	0.18	0.08	0.57	0.104
TiO_2	2.21	2.40	0.03	1.728
Cr_2O_3	/	0.06	/	0.0251
Fe_2O_3	2.14	5.54	2.20	9.635
ZnO	/	0.03	/	0.019
SrO	/	0.05	/	0.0049
ZrO_2	/	0.08	/	0.06185
MnO	/	0.75	1.78	0.138
V_2O_5				0.0398
Rb_2O				0.0044
CuO				0.008
NiO				0.0106
LOI	10.25	31.67	1.2	3.10

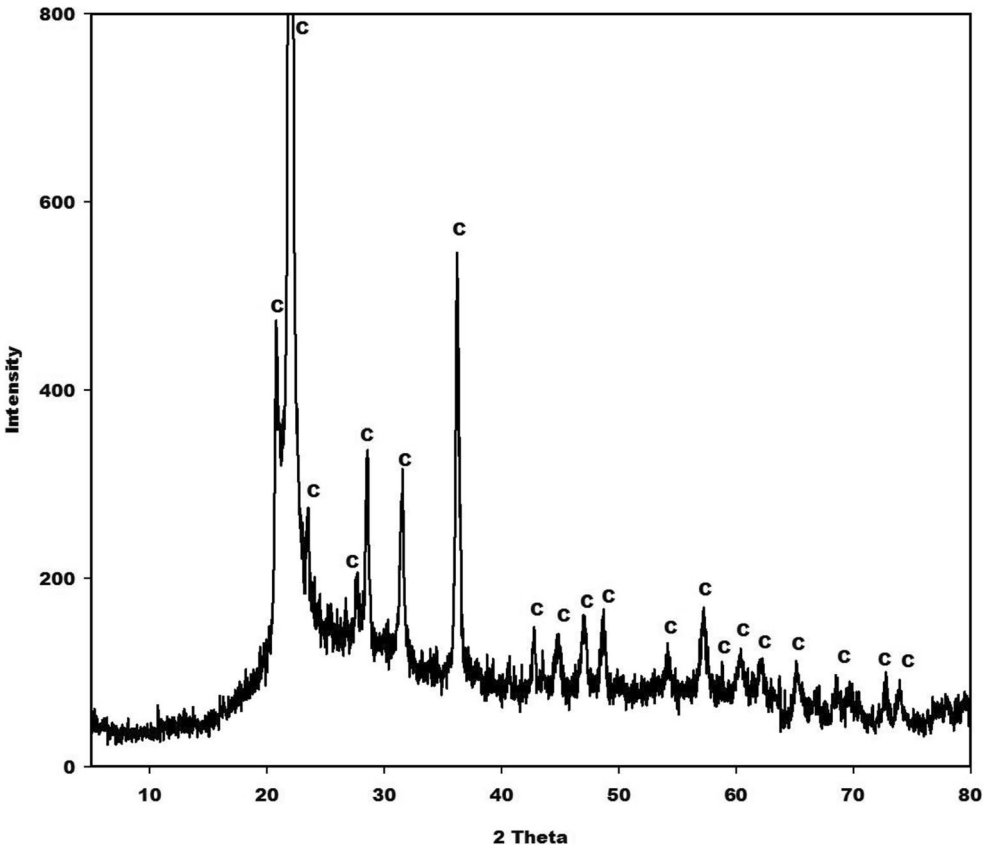

Fig. 1 X-ray pattern of rice husk ash, RHA. C denote peaks of cristobalite

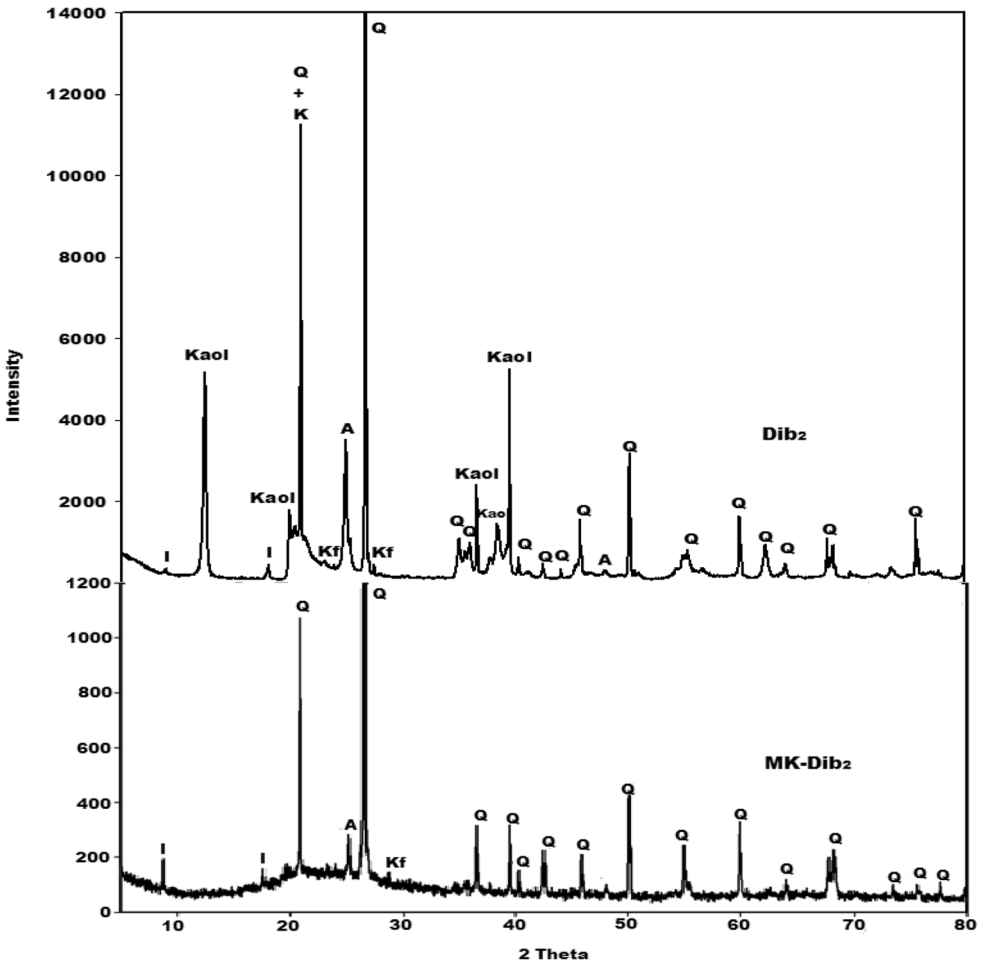

Fig. 2 X-ray patterns of kaolin, Dib_2. Kaol, I, Kf, A and Q denote peaks of kaolinite, illite, K-feldspars, anatase and quartz, respectively

phosphoric acid for the synthesis of acid-based geopolymers [4–11]. These researchers are reported that the main phase present in the network is poly(phospho-siloxo) and the mechanism has been tremendously described by Davidovits [12]. Whereas, those prepared in the alkaline condition depend on the molar ratio Si/Al in the network. For example, when the molar ratio Si/Al in the network is 1.0, the main phase is called poly(sialate). For the molar ratios, Si/Al equals 2.0 and 3.0, the main amorphous phases which are prevailing in the structures of the final products are poly(sialate-siloxo) and poly(sialate-disiloxo), respectively. The properties of the geopolymer materials prepared in alkaline medium and acidic medium (phosphoric acid) depend on the raw aluminosilicate used [10, 13]. The findings work of Bewa et al. [13] indicates that the presence of higher iron oxide, amorphous silica and quartz content in the raw aluminosilicate material affect positively the compressive strengths of acid-based geopolymers. In the same way, Banenzoué et al. [10] reported that the pure aluminosilicate material is not suitable for the synthesis of acid-based geopolymer materials. It is worth mentioning that the aluminosilicate sources generally used for the synthesis of geopolymer materials are composed of the amorphous phases associated with crystalline minerals. The amorphous phase is mainly constituted of silica and alumina associated with sometimes amorphous iron oxide and so on. The crystalline phases which to go with the amorphous phase or glass phase generally observed depend on the raw aluminosilicate used. The raw aluminosilicate sources could be a by-product of the metallurgical industry and thermal power plants such as blast furnace slag and fly ash, respectively. It exists also natural materials like volcanic scoria, laterite, kaolin, etc. In order to increase the reactivity of certain materials, for example, kaolin was calcined at about 700 °C [14] and laterite or indurated laterite was heated at about 600 °C [15]. Concerning the natural aluminosilicates, all the Cameroonian territory is constituted of deposits of kaolins [16], laterites [17] and volcanic scoria [18, 19]. Bewa et al. [13] reported that there are aluminosilicate sources that are rich in amorphous silica and others rich in crystalline silica. Silica is among the most common mineral in the earth's area. This mineral is also denoted silicon dioxide [20] and it can have an amorphous and crystalline structure. The most common form of

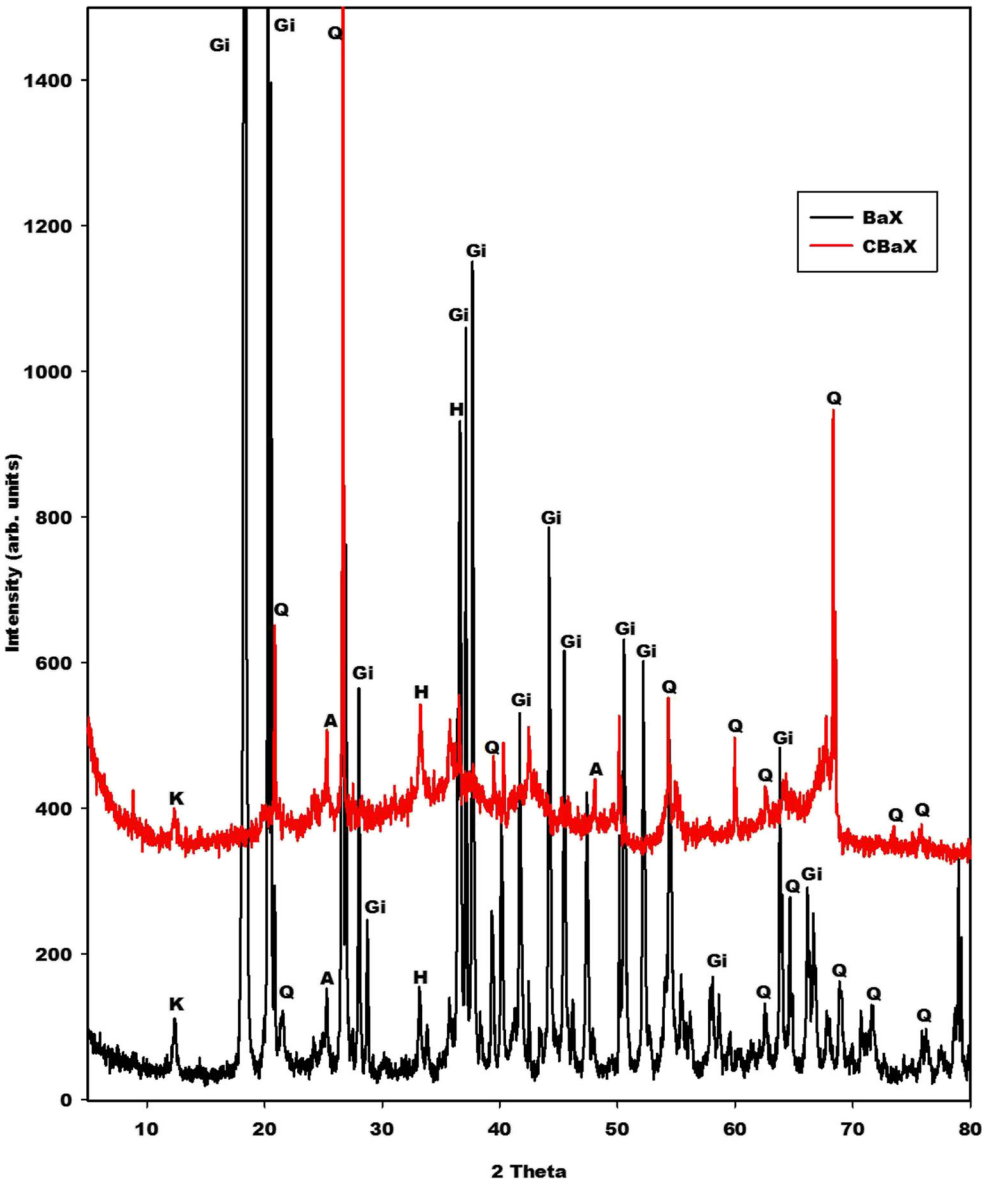

Fig. 3 X-ray patterns of bauxite (BaX) and calcined bauxite (CBaX). K, Gi, Q, A and H denote peaks of kaolinite, gibbsite, quartz, anatase and hematite, respectively

crystalline silica generally present in the aluminosilicate material is called quartz. It is important to note that this quartz is nearly chemically inert contrary to the amorphous one which has a great reactivity for example in the alkaline solution. This could be related to the fact that quartz features a lower hydroxyl group (OH) content. Whereas, the amorphous ones like silica fume, precipitated silica and silica from crops products such as rice husk ash, sugarcane bagasse ash and wheat husk ash have a huge hydroxyl groups content [21–23]. It is important to note that the achievement of the amorphous silica from these crops materials depend on the calcination temperature. Concerning bauxite, Nguimatsia and Yongue [24] reported that bauxite was found in the Western region of Cameroon more

Table 2 Mixed design of the geopolymer materials from metakaolin

Samples ID	Metakaolin (g)	Calcined bauxite (g)	Chemical reagent (g)	Calcined bauxite/metakaolin
GMK0	250	0	187.5	0
GMK25	250	25	187.5	0.1
GMK50	250	50	187.5	0.2
GMK75	250	75	210.8	0.3
GMK100	250	100	227.5	0.4

Table 3 Mixed design of the geopolymer materials from Waste fired brick

Samples ID	Waste fired brick (g)	Calcined bauxite (g)	Chemical reagent (g)	Calcined bauxite/waste fired brick
GWB0	250	0	187.5	0
GWB25	250	25	227.5	0.1
GWB50	250	50	227.5	0.2
GWB75	250	75	210.8	0.3
GWB100	250	100	227.5	0.4

specifically in the locality of Fongo Tongo. Little deposit of this alumina ore is found as well in the locality of Nkongsamba in the Littoral region of Cameroon. The huge deposit is located at Minim-Martap in the department of Vina in the Adamawa region of Cameroon [25] which could be among the most important in the world. This has been confirmed by the company Canyon Resources which estimates about 900 million tonnes of bauxite with about 250 million tonnes of " very high grade " bauxite at the Minim-Martap. Another alumina source is red mud which is bauxite residue (waste) that originated in the processing of bauxite into aluminium [26]. The investigation of the influence of alumina in geopolymerization has been done by several researchers. For example, Le et al. [27] investigated the role of active silica and alumina in geopolymerization by varying the molar concentration of NaOH. They reported that the active oxides can participate in the geopolymer reactions, i.e. silicon atoms can be linked by a "bridging" oxygen (Si-O-Si) to form independent polymer chains, while aluminum atoms can only replace silicon atoms in Si-O-Si polymer chains to form Si-O-Al [27]. Zidi et al. [28] studied the influence of Al_2O_3 nanoparticles on the mechanical, structural and thermal properties of geopolymers. They concluded that the addition of Al_2O_3 nanoparticles to alkali-activated geopolymer materials induces more nucleation sites leading to the formation of more sialate bonds in the system. Phoongernkham et al. [29] concluded that the incorporation of nano-alumina has a more effective influence on the structural and mechanical properties of geopolymer

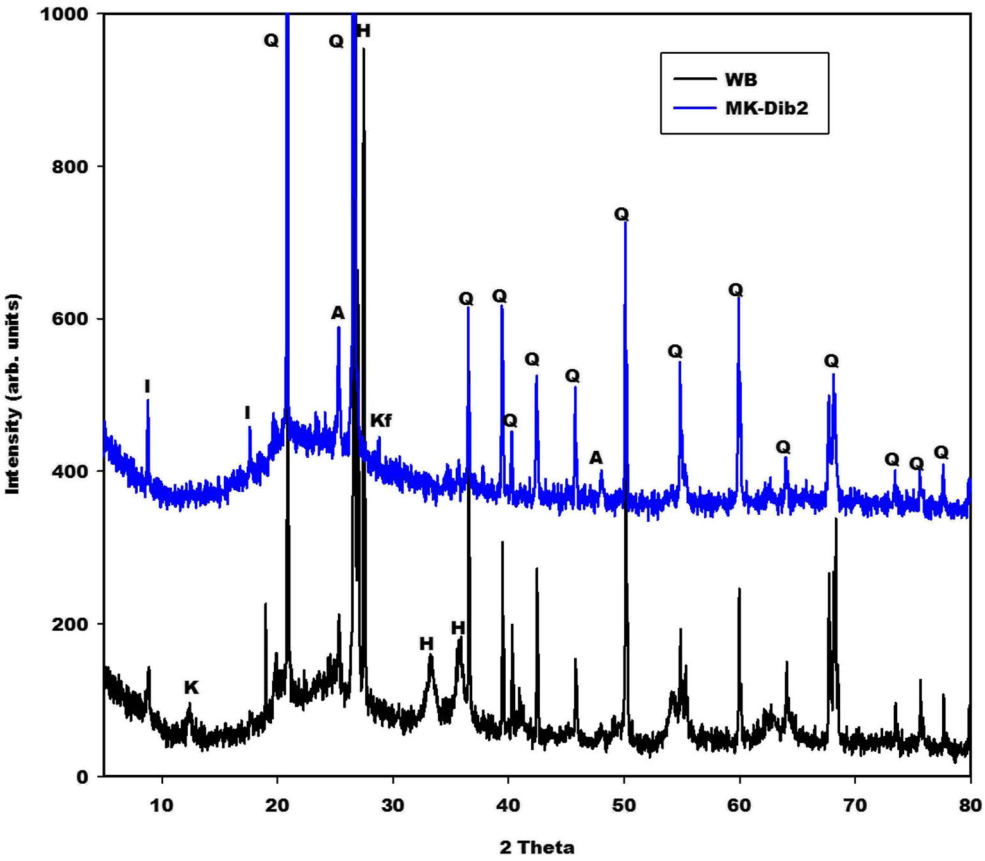

Fig. 4 X-ray patterns of waste fired brick (WB) and metakaolin (MK-Dib_2). I, K, Kf, A and H denote peaks of illite, kaolinite, K-feldspar, anatase and hematite, respectively

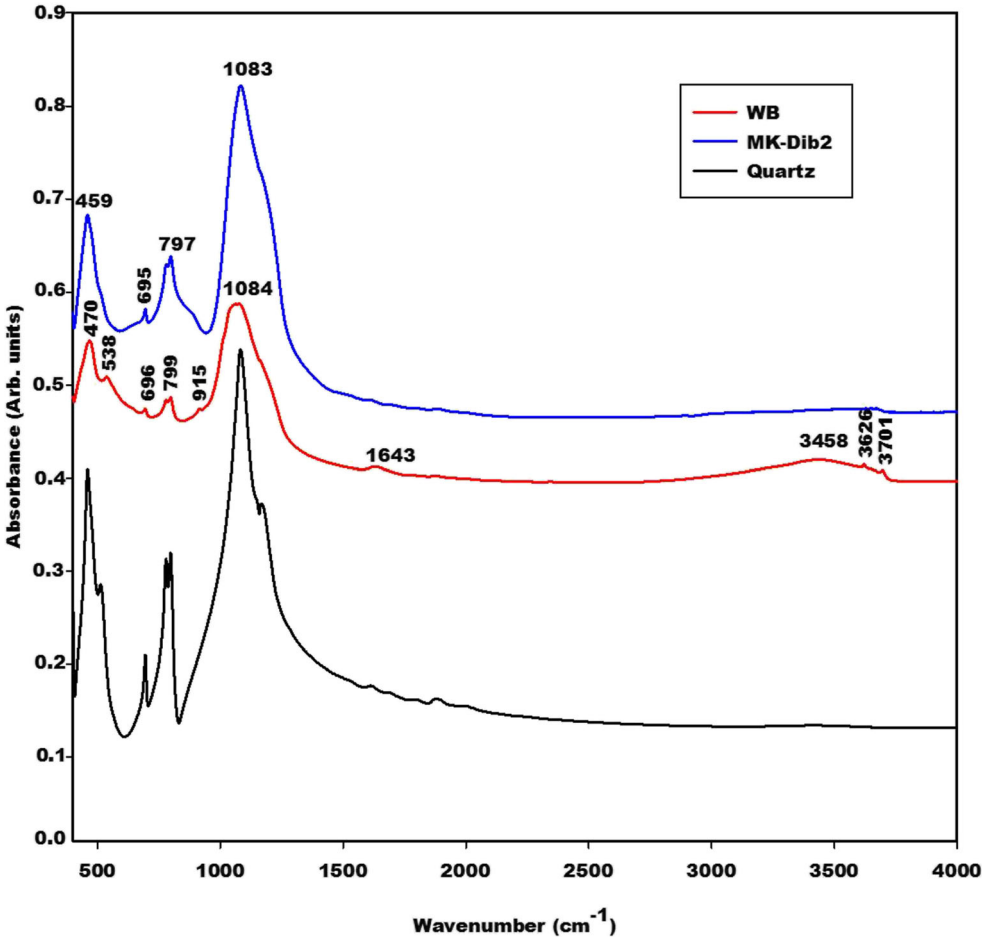

Fig. 5 Infrared spectra of waste fired brick (WB) and metakaolin (MK-Dib_2)

materials than nano-silica. Zheng et al. [30] and Duxson et al. [31] reported that lower Si/Al ratio results in a larger surface area of geopolymer beneficial for adsorption capacity. Tchakouté et al. [32] compare the compressive strengths of geopolymer cement from metakaolin and volcanic ash using amorphous alumina as a supplementary Al source. They concluded that 20 and 40% of Al_2O_3 lead to 18.1 and 32.4% increases in the compressive strengths of geopolymer cements from metakaolin and volcanic ash, respectively. The findings work of Bewa et al. [13] indicated that waste fired brick and metakaolin used in the present work contain a higher amorphous silica and quartz content, respectively. The properties of the geopolymer materials from the addition of semi-crystalline alumina on these aluminosilicates are not yet elucidated.

The main target of this work is to investigate the behaviour of the semi-crystalline alumina added to the aluminosilicates rich in amorphous and crystalline silica during the geopolymerization process. The hardener used as an alkaline reagent in this work is a sodium waterglass from rice husk ash containing a molar ratio SiO_2/Na_2O equal to 1.6. The behaviour of the semi-crystalline alumina added to the aluminosilicates rich in amorphous and crystalline silica during the geopolymerization process is investigated by the measurement of the compressive strengths. The structural properties have been studied using X-ray diffractometry and infrared spectroscopy. The quartz and amorphous phases content has been also estimated. The microstructure has been monitored using the scanning electron microscope coupled with the energy dispersive X-ray analysis.

2 Materials and Experimental Methods

2.1 Materials

The aluminosilicates rich in silica used in this investigation are waste fired brick and kaolin. The alumina and silica sources are bauxite and rice husk ash, respectively. Waste fired brick has been provided by the Local Materials Promotion Authority (MIPROMALO) situated in the Centre region of Cameroon. Kaolin was harvested from Dibamba in the

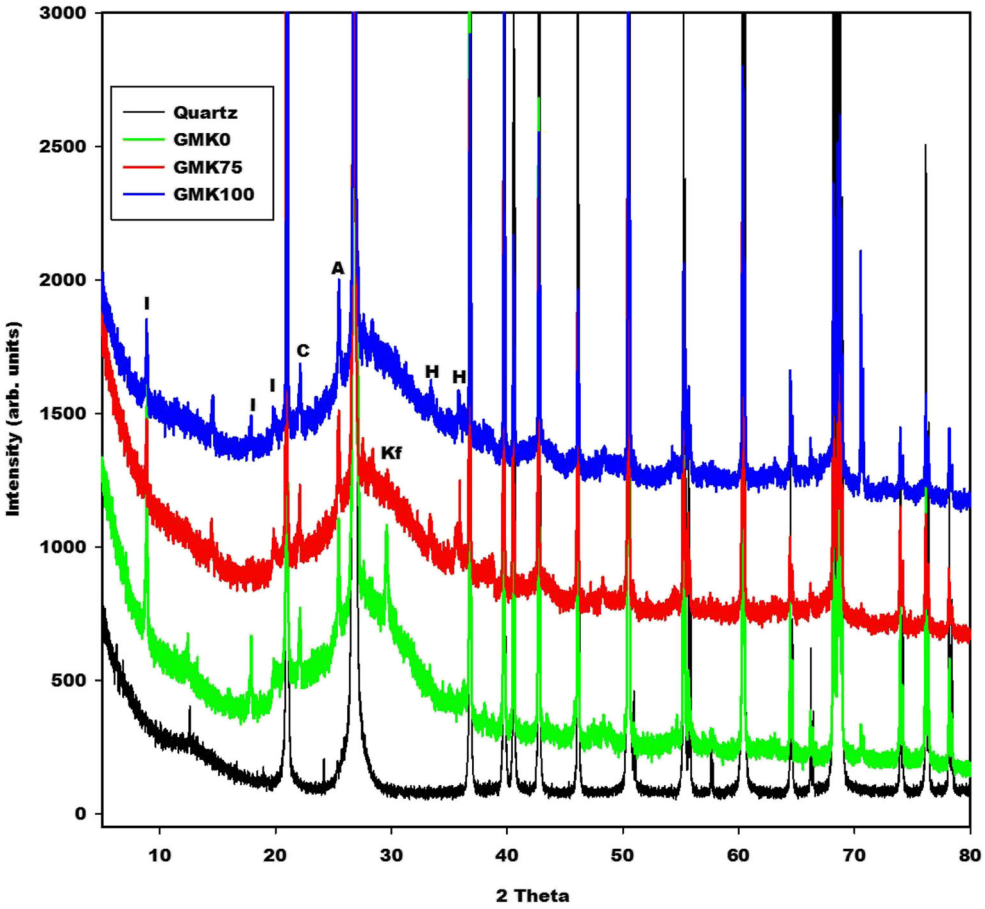

Fig. 6 X-ray diffractograms of geopolymer materials from metakaolin (GMK0, GMK75 and GMK100) and quartz. I, C, Kf, A and H denote peaks of illite, cristobalite, K-feldspar, anatase and hematite, respectively

Littoral region of Cameroon. Bauxite was collected from Mini-Martap in the Adamawa region of Cameroon. Rice husk ash was provided by Upper Nyoung Valley Development Association (UNVDA). This company is situated in Ndop in the Department of Ngoketundjia, Region of North-West (Cameroon). The silica source with white colour has been calcined in the open air for 4 h by UNVDA before being ground in small pieces. Once collected, waste fired brick, kaolin and bauxite were first dried in air for 24 h and then broken into small pieces using a hammer. Each piece of waste fired brick, kaolin, bauxite and rice husk ash were pulverized separately in the ball mill (MGS, Srl) for 45 min. The resultant powder of each material was sieved through 125 μm and the obtained powders of waste fired brick, kaolin, bauxite and rice husk ash were denoted WB, Dib_2, BaX and RHA, respectively. The powders of kaolin and bauxite were transformed to metakaolin (for kaolin) and semi-crystalline alumina (for bauxite) by the calcination at 700 °C (for 4 h) and 600 °C (for 2 h), in order to obtain the powders, denoted MK-Dib_2 and CBaX, respectively. The heating and cooling rate of 5 °C/min are maintained during the calcination of these materials. NaOH pellet was provided by the laboratory-grade granules (96 wt%, Sigma Aldrich, Italy). The chemical compositions of kaolin (Dib_2), rice husk ash (RHA), bauxite (BaX) and waste fired brick (WB) have been reported in Table 1. It is important to mention that kaolin and rice husk ash have been described by Melele et al. [33]. The X-ray pattern of rice husk ash (RHA) is displayed in Fig. 1 and those of kaolin (Dib_2) is presented in Fig. 2. The X-ray patterns of bauxite (BaX) and calcined bauxite (CBaX) are depicted in Fig. 3. Bauxite and waste fired brick have been studied by Tchamba et al. [25] and Beleuk à Moungam et al. [34], respectively. The bauxite and semi-crystalline alumina is already described by Moudio et al. [35]. Commercial quartz from Fluka was used as reference crystalline silica.

2.2 Experimental Methods

2.2.1 Preparation of Sodium Waterglass from Rice Husk ash

Sodium waterglass containing a molar ratio SiO_2/Na_2O equal to 1.6 has been prepared using rice husk ash and sodium hydroxide. For its preparation, water was added to the sodium

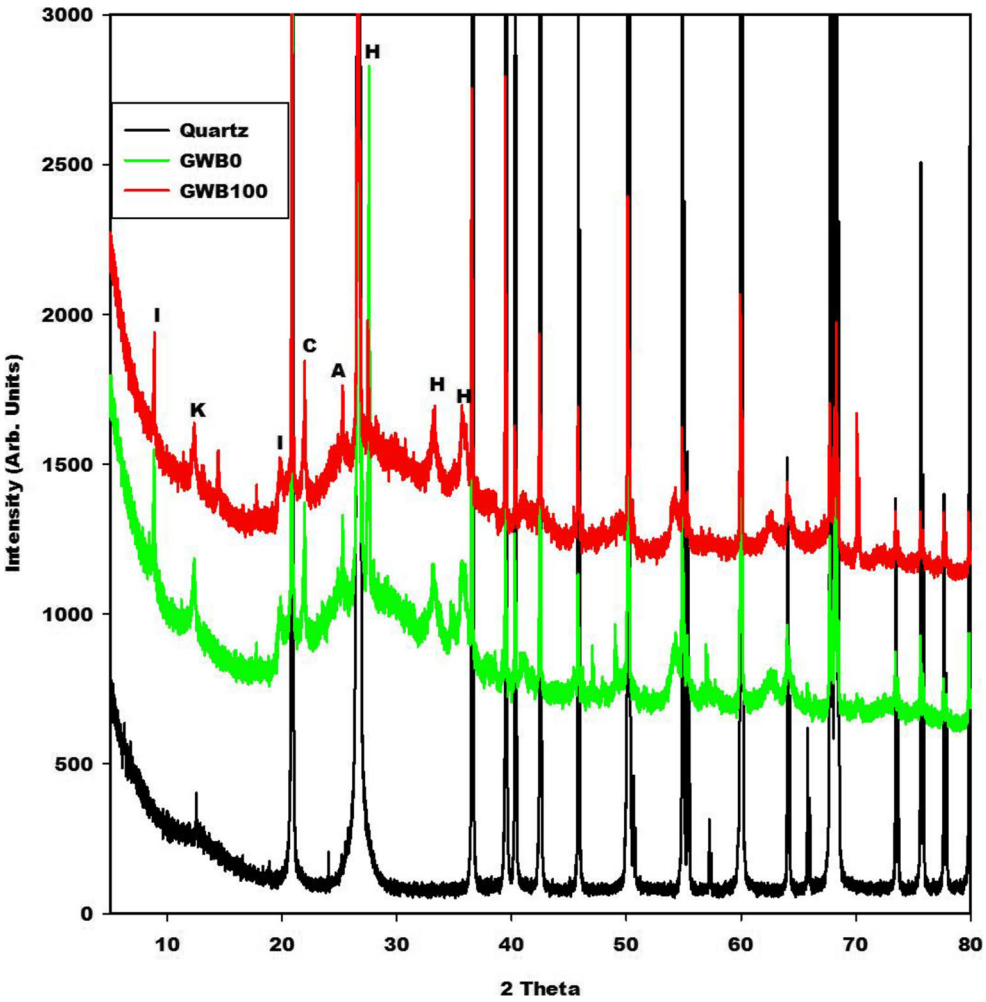

Fig. 7 X-ray diffractograms of geopolymer materials from waste fired brick (GWB0 and GWB100) and quartz. I, C, K, A and H denote peaks of illite, cristobalite, kaolinite, anatase and hematite, respectively

hydroxide pellet in order to obtain sodium hydroxide solution. The whole was mixed with rice husk ash. The mixture was heated for about 1 h at 100 °C using a magnetic stirrer to obtain sodium waterglass.

2.2.2 Synthesis of Geopolymer Materials

Geopolymer materials were synthesized by adding firstly metakaolin or waste fired brick to calcined bauxite. The mass ratios of the raw materials (calcined bauxite, metakaolin and waste fired brick) designed as calcined bauxite/metakaolin or calcined bauxite/waste fired brick are equal to 0, 0.1, 0.2, 0.3 and 0.4. The prepared sodium waterglass was added to each aforementioned mixture and blended for about 5 min to obtain the fresh pastes of geopolymer materials for each composition. The obtained fresh pastes were moulded in the cubic moulds (40 mm) and vibrated for about 2 min using a vibrating table. The moulded pastes were covered with plastics and left in the laboratory for 24 h before demoulding. Afterwards, the

Table 4 Amorphous and crystalline phase contents (wt%)

Specimens	GMK0	GMK75	GMK100	GWB0	GWB100
Quartz (wt%)	50	57	37	31	32
Other crystalline phases (wt%)	14	1.6	19	28	22
Total crystalline phases (wt%)	64	58.4	56	59	54
Amorphous phases (wt%)	36	41.6	44	41	46

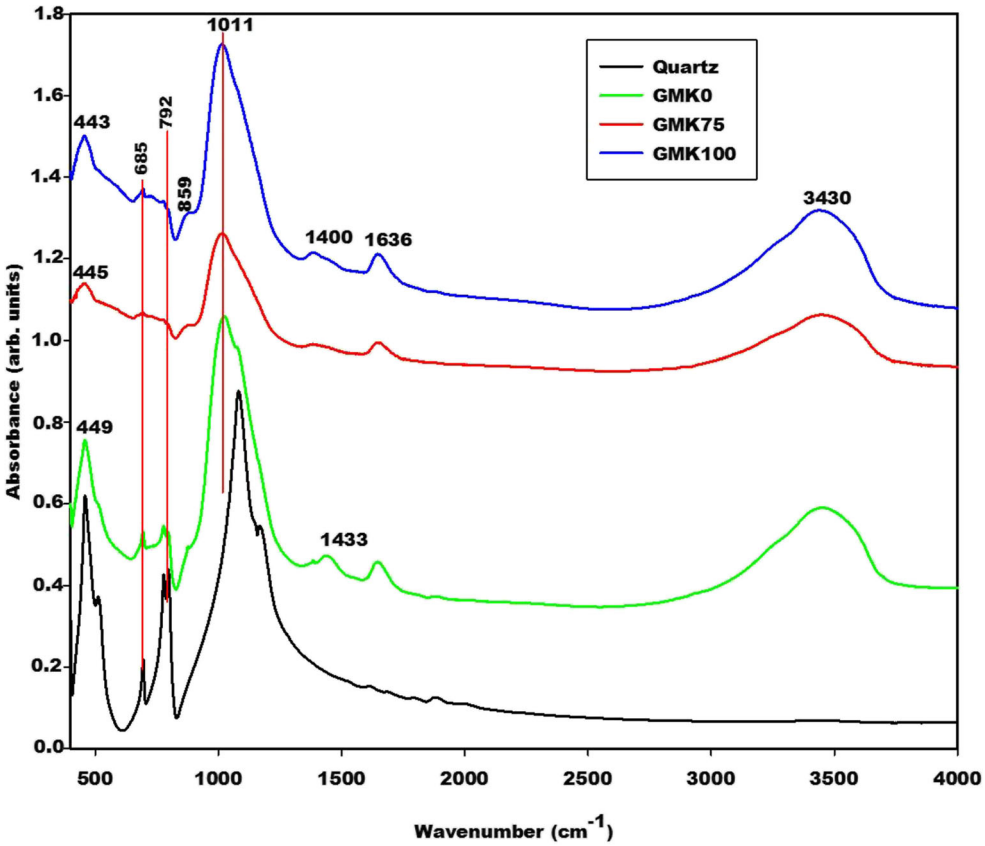

Fig. 8 Infrared spectra of geopolymer materials from metakaolin (GMK0, GMK75 and GMK100) and quartz

demoulded specimens were maintained at room temperature of the laboratory for 28 days before testing their compressive strengths. Geopolymer materials from the mass ratios calcined bauxite/ metakaolin equals to 0, 0.1, 0.2, 0.3 and 0.4 are denoted GMK0, GMK25, GMK50, GMK75 and GMK100, respectively. Whereas those from these mass ratios calcined bauxite/waste fired brick are called GWB0, GWB25, GWB50, GWB75 and GWB100, respectively. The mixed design of the geopolymer materials from metakaolin and waste fired brick have been reported in Tables 2 and 3, respectively.

2.2.3 Methods of Characterisation of Raw Materials and Metakaolin-based Geopolymer Cements

The behaviour of the semi-crystalline alumina added to the aluminosilicates rich in amorphous and crystalline silica during the geopolymerization process was assessed by measuring their compressive strengths. The structural properties of the geopolymer materials have been investigated on the powders using an X-ray diffractometer and infrared spectrometer apparatus. The microstructure has been studied by the observation of the fragments on the geopolymer materials using a scanning electron microscope (SEM). The spectra of different zones of the selected specimens were recorded using the EDS analysis during the observation of fragments on the microscope.

The compressive strengths of the prepared geopolymer materials were measured on an automatic hydraulic press with a 250 kN capacity (Impact Test Equipment Limited, UK KA20 3LR) according to the DIN 1164 standard using a loading rate kept constant at 0.500 MPa/s. The fragments of the selected compositions such as GMK0, GMK75, GMK100, GWB0 and GWB100 after compressive strengths testing were collected. One part was used for SEM observations and the others were finely ground in a porcelain mortar. The obtained powders were used for registering their X-ray diffractograms and infrared spectra.

The X-ray patterns of the selected geopolymer materials and quartz were performed on a Bruker D8 Advance equipped with LynXeye XE T detector detecting CuKα1,2 in Bragg Brentano geometry. The range between 5 and 80° (2θ) was measured for 1 h per sample in steps of 0.01°. The crystalline

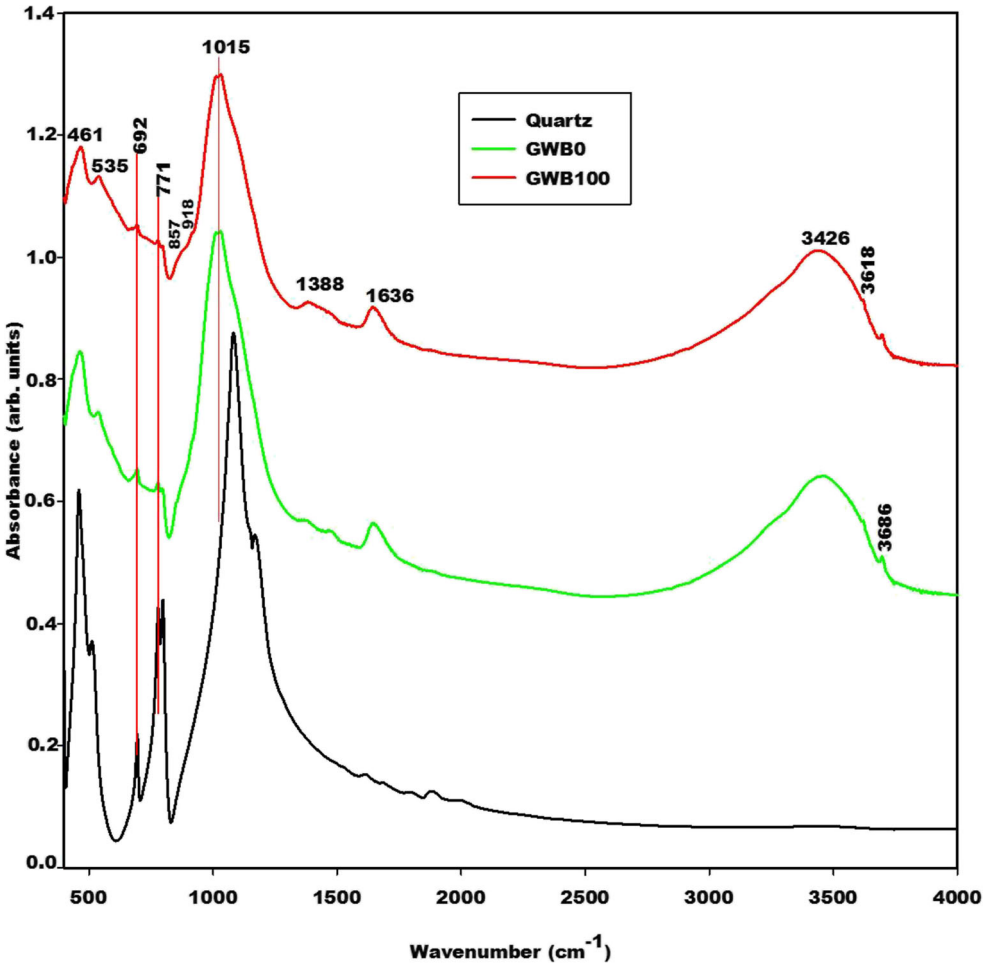

Fig. 9 Infrared spectra of geopolymer materials from waste fired brick (GMK0, GMK75 and GMK100) and quartz

phases present in the structure of each specimen were identified using X'Pert HighScore Plus software. Opus-Software was used to calculate the intensities. They were done by simply making 1st baseline correction to get the total intensity (subtract instrumental scattering) = S(tot), the baseline correction by subtracting the amorphous and instrumental part (S(Cryst) and finally integrating the intensity of all Quartz peaks (S(Qz).

$$S(\text{amorphous}) = S(\text{Tot}) - S(\text{cryst}) \text{ and } S(\text{cryst}) = S(\text{Qz}) + \text{rest}.$$

The infrared spectroscopy analysis of the selected geopolymer materials were determined using the KBr method where about 200 mg of KBr was mixed with around 1 mg of the sample. The whole was mixed in an agate mortar and pressed at 100 kN using a hydraulic press (ENERPAC P392, USA). The obtained pellets were used to record the spectra with the resolution of 2 cm^{-1} and 16 scans using a Bruker Vertex 80v. The data were collected using OPUS software.

The selected fragments of geopolymer materials after gold/palladium-coating were used for the micrograph image observations coupled with microanalysis using energy dispersive X-ray analysis (EDS). The observation of the selected fragment of the microscope was done on a LEICA EM ACE600 with an acceleration voltage of 20.0 kV.

3 Results and Discussion

3.1 Characterisation of Starting Materials

3.1.1 X-ray Patterns

The X-ray powder diffractograms of waste fired brick (WB), metakaolin (MK-Dib$_2$) and quartz as reference are reported in Fig. 4. Both X-ray patterns display the peaks of illite, anatase and quartz. In addition to these crystalline minerals, the main peak of K-feldspar is observed on the diffractogram of

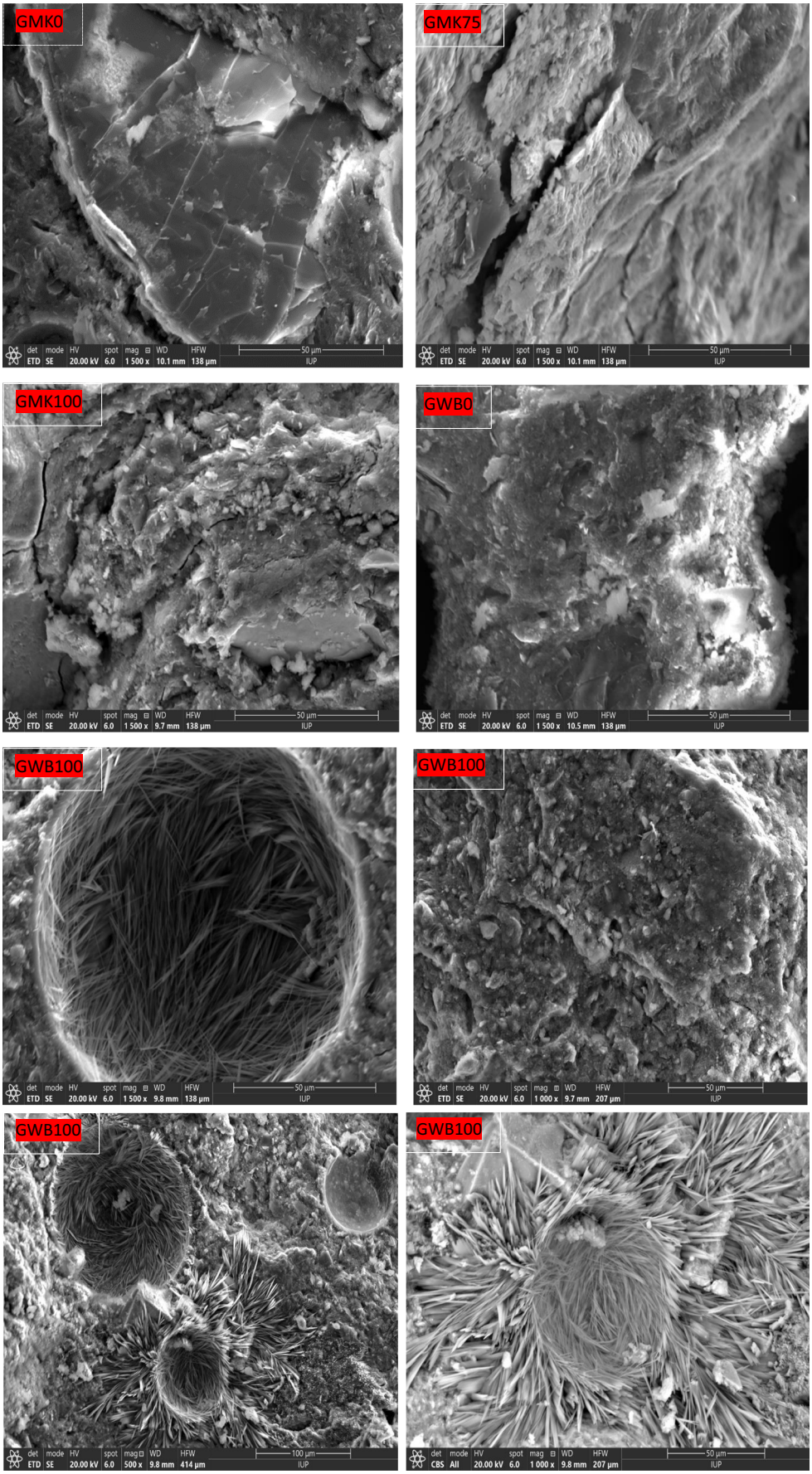

Fig. 10 Micrography images of the selected geopolymer materials (GMK0, GMK75, GMK100, GWB0 and GWB100)

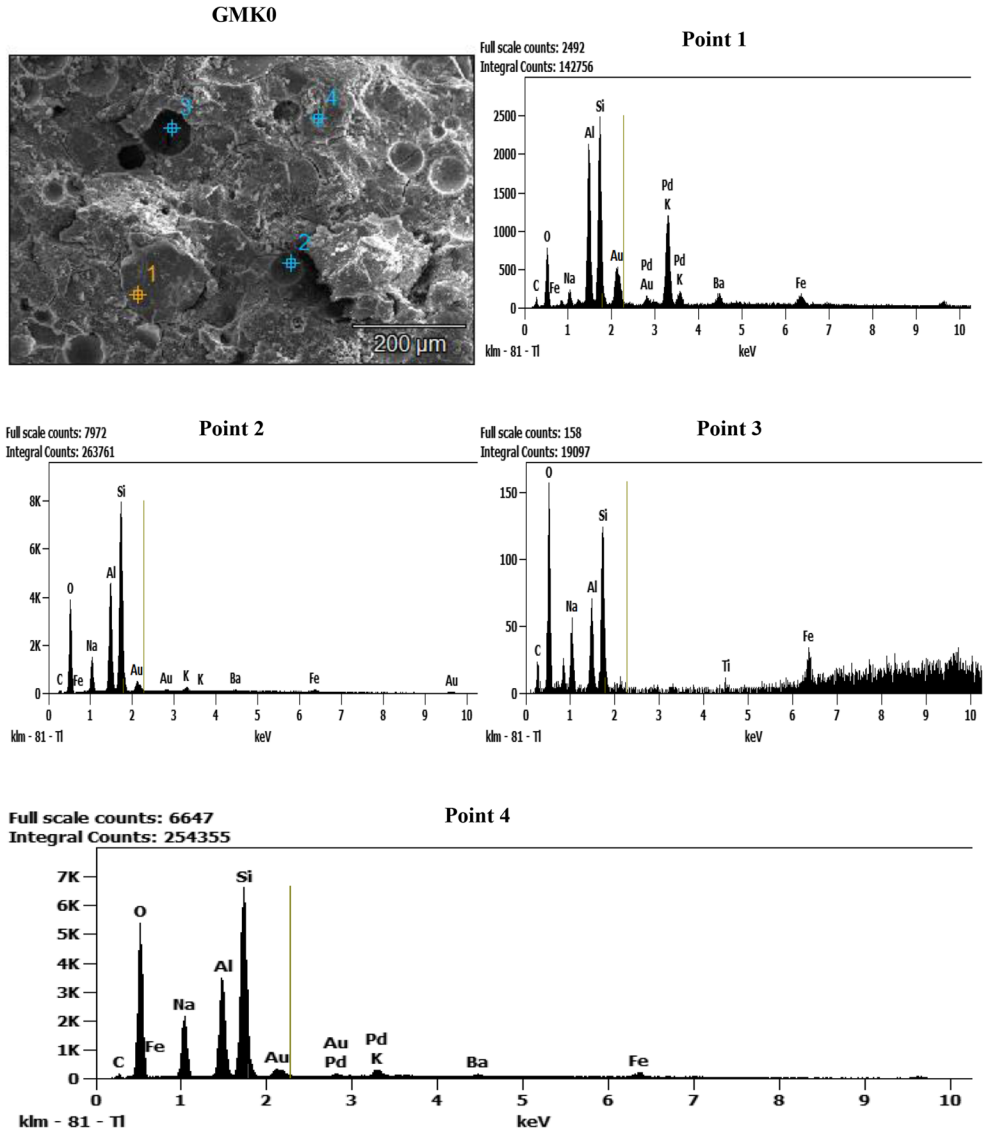

Fig. 11 Microanalysis investigation (EDS) of the selected geopolymer materials (GMK0, GMK75, GMK100, GWB0 and GWB100)

metakaolin, whereas, the one of waste fired brick indicates the peaks of hematite and residual kaolinite. The broad peaks of hematite observed at about 33.12 and 35.62 °(2θ) could be related to the presence of semi-crystalline hematite [13]. Both diffractograms likewise illustrate the broad hump structure between 15 and 38 °(2θ) corresponding to the formation of metakaolinite (amorphous aluminosilicate phase) in the structure of waste fired brick and metakaolin [13, 31].

3.1.2 Infrared Spectra

Figure 5 illustrates the infrared spectra of waste fired brick (WB), metakaolin (MK-Dib$_2$) and quartz as reference. The absorption bands situated at 470 and 459 cm^{-1} on the spectra of waste fired brick and metakaolin, respectively, are assigned to the bending vibration modes of siloxane (Si-O-Si) bonds [36]. The band that appears at 538 cm^{-1} on the spectrum of waste fired brick is associated with the vibration modes of Fe-O of hematite. This corroborates the X-ray diffractogram of WB which shows the peaks of hematite. The absorption bands at 696 − 695 and 799 − 797 cm^{-1} indicated the presence of quartz [37]. Those at 915, 3626 and 3701 cm^{-1} on the spectrum of waste fired brick are attributed to the residual kaolinite. The presence of kaolinite is confirmed by the appearance of the main reflection peak of kaolinite at around 12.2° (2θ) on the XRD pattern of WB (Fig. 5). The absorption bands with low intensity at about 1643 and 3458 cm^{-1} observed on the spectrum of waste fired bricks are attributed to the vibration modes of H-O-H and O-H of water molecules and silanol groups, respectively. It can be seen that the main absorption bands at 1083 cm^{-1} for metakaolin and 1084 cm^{-1} for waste fired brick are

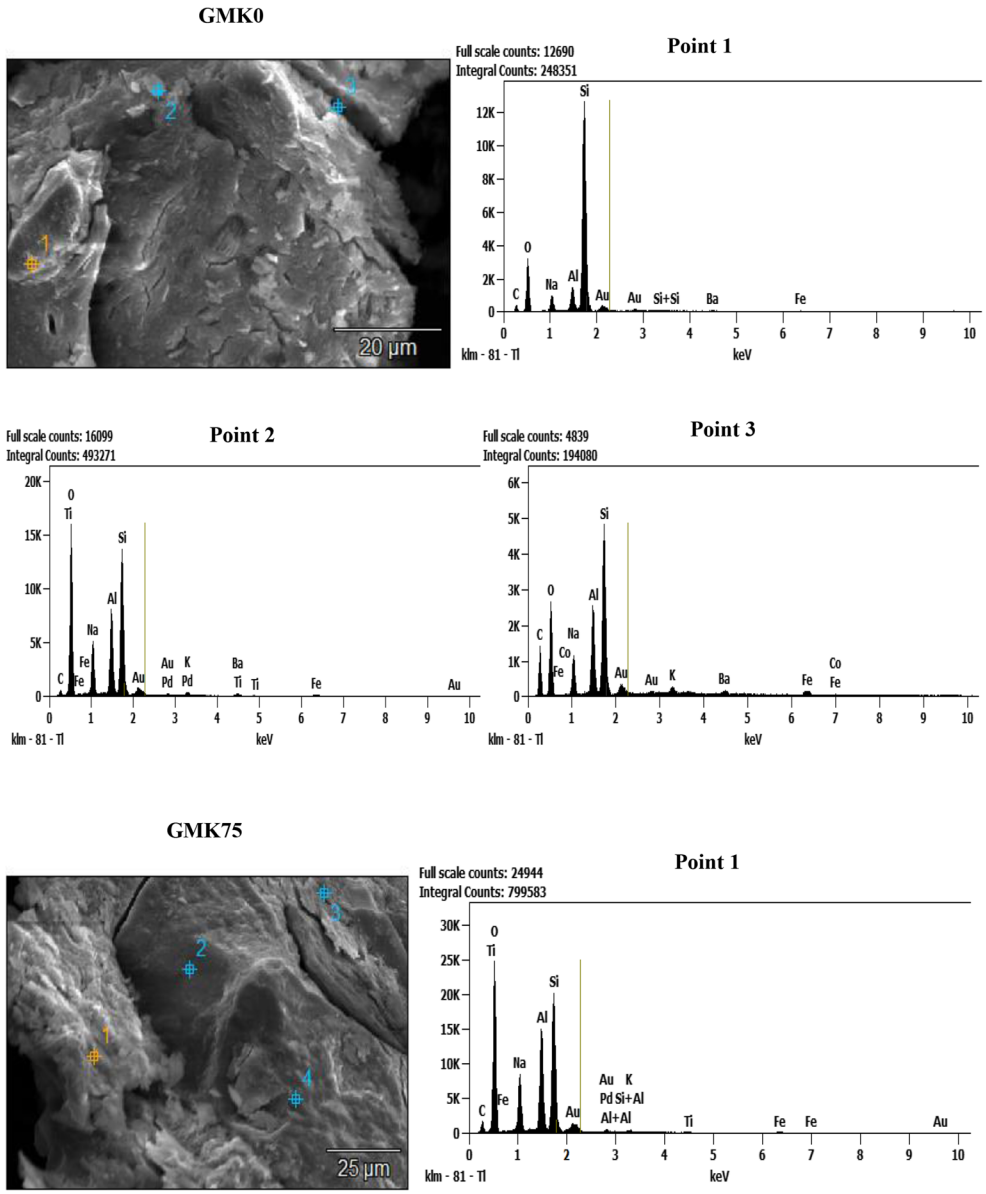

Fig. 11 (continued)

narrow and broad, respectively. Compared to the spectrum of quartz, it is obvious that the narrow main band observed on the spectrum of metakaolin could be attributed to the higher quartz content and the broad one on the spectrum of waste fired brick is assigned to the higher amorphous phase content. Regarding the chemical composition of metakaolin and waste fired brick reported in Table 1, it can be seen that metakaolin and waste fired brick contain 59.60 and 60.98 wt% of silicon dioxide (SiO_2), respectively. The combination of the chemical compositions and the infrared spectra results of these raw materials leads us to conclude that metakaolin is rich in crystalline silica (quartz) and waste fired brick is rich in amorphous silica. The higher quartz content in the structure of metakaolin is also confirmed by the higher intensities of the absorption bands that appear at 459, 695 and 797 cm^{-1} (Fig. 5). It is important to indicate that the absorption band values present on the spectra of MK-Dib_2 and WB have been described by Melele et al. [31] and Bewa et al. [13], respectively.

3.2 Characterisation of Geopolymer Materials

3.2.1 X-ray Diffractograms, Crystalline and Amorphous Phases Content

Figures 6 and 7 display the X-ray patterns of the selected geopolymer materials from metakaolin (GMK0, GMK75

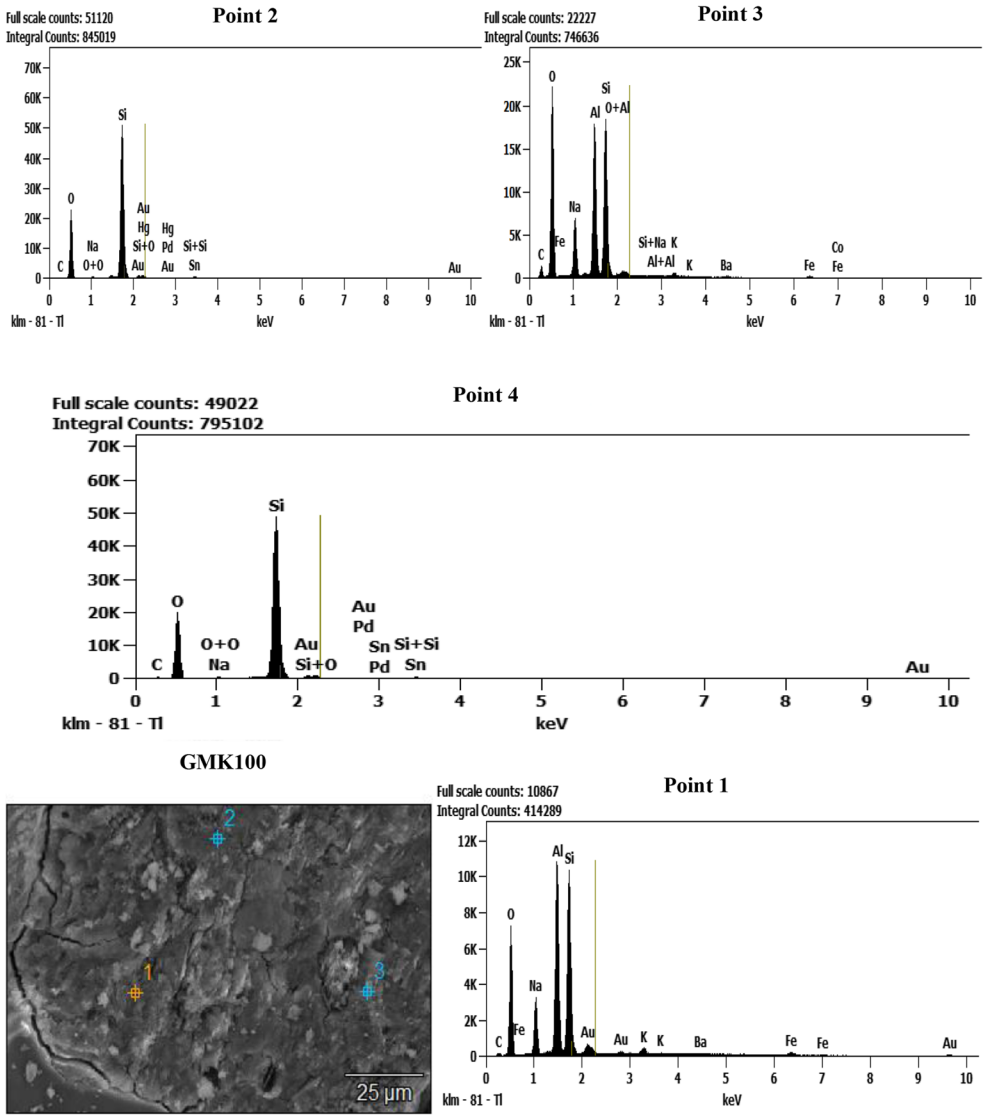

Fig. 11 (continued)

and GMK100) and waste fired brick (GWB0 and GWB100), respectively, with quartz reference. The diffractograms of all geopolymer materials show the peaks of illite, anatase, hematite, cristobalite and quartz. The cristobalite presented on the X-ray patterns of geopolymer materials is come from sodium waterglass indicating that this mineral does not dissolve in an alkaline medium during the preparation of sodium waterglass from rice husk ash. The presence of hematite in the structure of geopolymer materials from metakaolin after addition to the semi-crystalline alumina comes from calcined bauxite. In addition to these minerals, those from metakaolin indicate the peaks of K-feldspar while those from waste fired brick exhibit the peak of residual kaolinite. Besides these crystalline phases, the X-ray patterns present the broad hump structure between 20 and 40 ° (2θ) corresponding to the formation of the binders in the structure of the final products. The presence of crystalline and amorphous phases in the structure of geopolymer materials indicate that these inorganic polymers are semi-crystalline materials.

The amount of the crystalline and amorphous phases contained in the structures of geopolymer materials, GMK0, GMK75, GMK100, GWB0 and GWB100, are presented in Table 4. It was observed that geopolymer materials, GMK0, GMK75 and GMK100 have 36, 41.6 and 44 wt% of amorphous phase content, respectively. The quartz content in the aforementioned geopolymer materials are 50, 57 and 37 wt%, respectively. Whereas, those from waste fired brick GBW0 and GBWB100 are 41 and 46 wt% of amorphous phases, respectively, and 31 and 32 wt% of quartz content, respectively. The specimens from metakaolin contain a higher quartz content compared to those from waste fired brick. It seems that the amorphous phases content increase with increasing

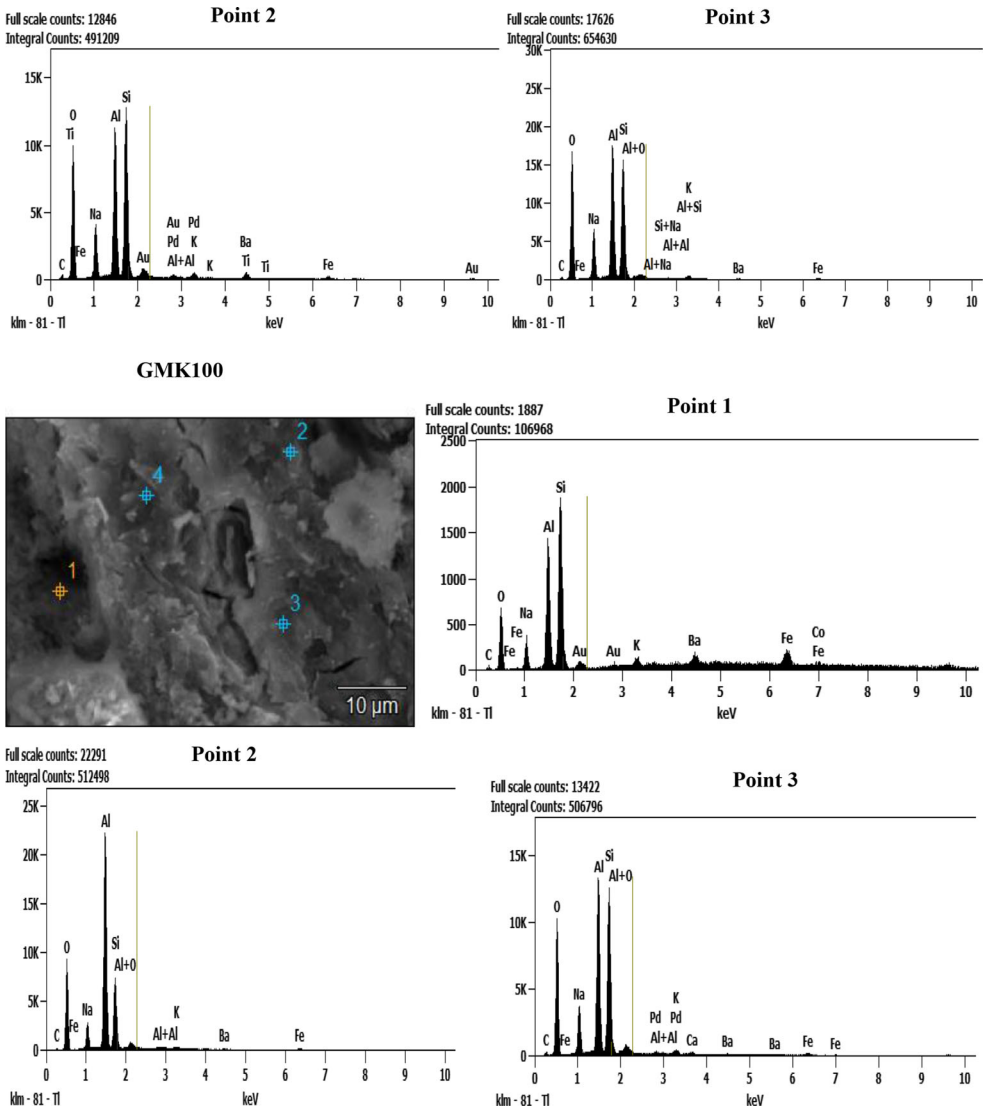

Fig. 11 (continued)

the mass ratios of calcined bauxite/metakaolin and calcined bauxite/waste fired brick. This could be related to the growing of the binder when the mass ratios of calcined bauxite/metakaolin and calcined bauxite/waste fired brick increase. The quartz content in the structure of geopolymer materials from waste fired brick is nearly the same value while the ones from metakaolin increase from 50 to 57 wt% when the mass ratios are ranging from 0 to 0.3. The increase of the quartz content could be related to the addition of calcined bauxite to metakaolin because the X-ray patterns of calcined bauxite show some peaks of this mineral (Fig. 3). The increasing of the mass ratios of calcined bauxite/metakaolin from 0.3 to 0.4 entails a decreasing the quartz content (from 57 to 37 wt%). This could indicate that some quartz particles involve in the geopolymerization process according to the findings work of Bewa et al. [13].

3.2.2 Infrared Spectra

Figures 8 and 9 depict the infrared spectra of geopolymer materials from the selected mass ratios calcined bauxite/metakaolin and calcined bauxite/waste fired brick, respectively associated with quartz. The adsorption bands ranging from 461 to 443 cm^{-1} on the spectra of GMK0, GMK75, GMK100, GWB0, GWG100 and the quartz reference are ascribed to the bending vibrations modes of Si-O bonds. The bending one of Fe-O on the spectra of GWB0 and GWB100 (Fig. 9) that appears at 535 cm^{-1} confirms the presence of hematite observed on the X-ray patterns (Fig. 7). The absorption bands appear at 685 and 792 cm^{-1} on the infrared spectra of GMK0, GMK75 and GMK100. Those observed at 692 and 771 cm^{-1} on the spectra of GWB0 and GWB100 are compared to the spectrum of quartz. It can be seen that these bands

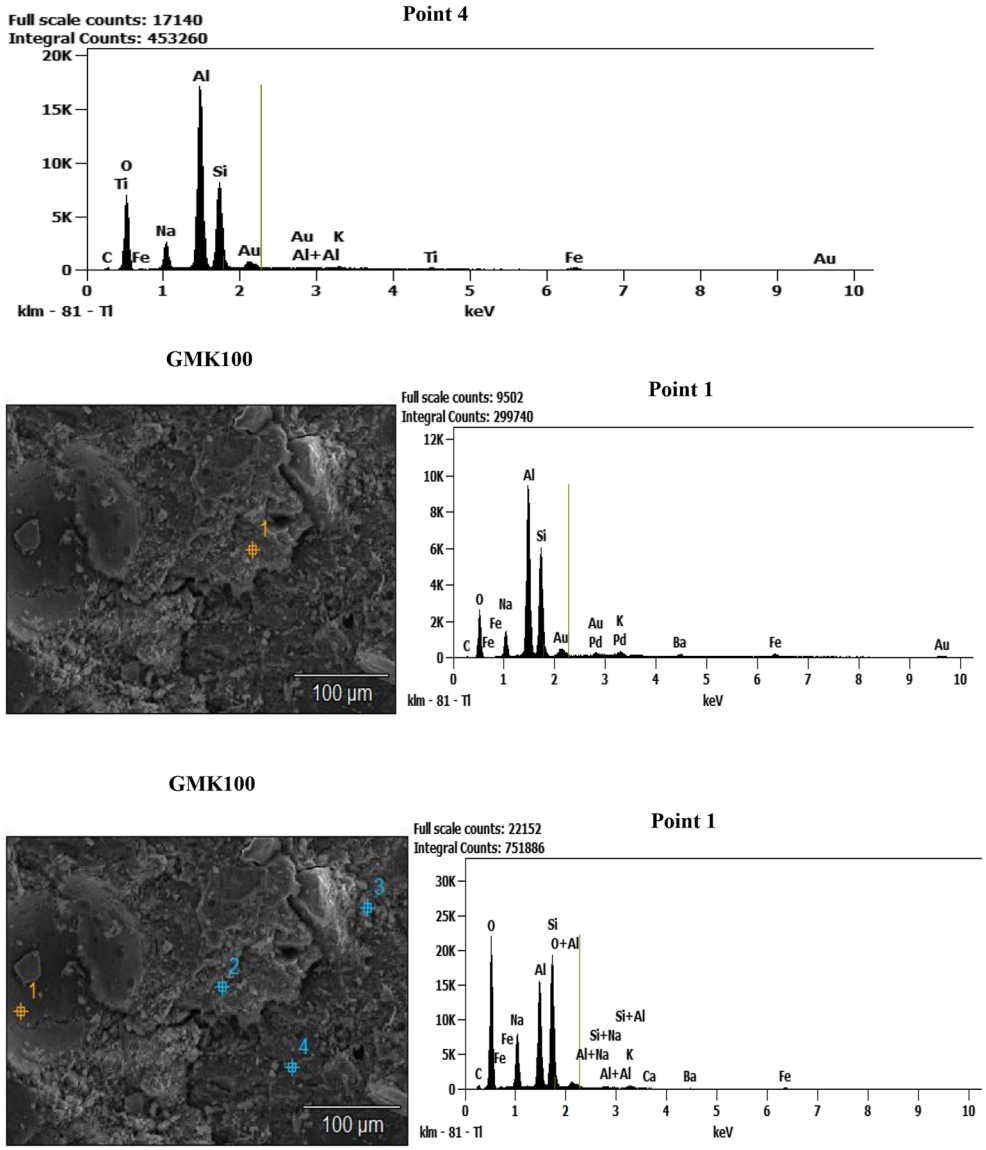

Fig. 11 (continued)

are attributed to the stretching vibration modes of Si-O bonds of quartz. The bands that appear between 859 and 857 cm^{-1} on the spectra GMK0, GMK75, GMK100 and GWG100 are assigned to the bending vibration modes of silanol groups (Si-OH). This band does not appears on the spectrum of GBW0 entailing the higher degree of polycondensation reaction. The main absorption band appears at 1011 cm^{-1} on the spectra of GMK0, GMK75 and GMK100, 1015 cm^{-1} on the spectra of GWB0 and GWB100. These bands that belong to the asymmetrical and symmetrical vibration modes of siloxane (Si-O-Si) and sialate (Si-O-Al) bonds appear at 1083 and 1084 cm^{-1} on the spectra of metakaolin ($MKDib_2$) and waste fired brick (WB), respectively (Fig. 4). This is due to the formation of 3D dimensional geopolymer materials [28]. The shift of these main bands compared to the ones of metakaolin and waste fired brick (Fig. 4) could be ascribed to the replacement of Si in Si-O-Si by Al leading to the formation of sialate bonds (Si-O-Al). According to Zidi et al. [28], this replacement offers more nucleation sites. The slight band at 918 cm^{-1} which is ascribed to the stretching vibrations of Al-OH bonds is observed on the spectrum of GWB100 leading to the low degree of geopolymerization process. This could indicate that the semi-crystalline alumina added to the waste fired brick does not take part in the geopolymerization process. The lower degree of the polycondensation reaction could also be confirmed by the higher intensity of the absorption band that appears at 1388 cm^{-1} on the spectrum of GWB100 compared to the one of GWB0. This band belongs to the C-O of Na_2CO_3 like the one ranging from 1433 to 1400 cm^{-1} on the spectra of GMK0, GMK75 and GMK100. The bands at 1636 and

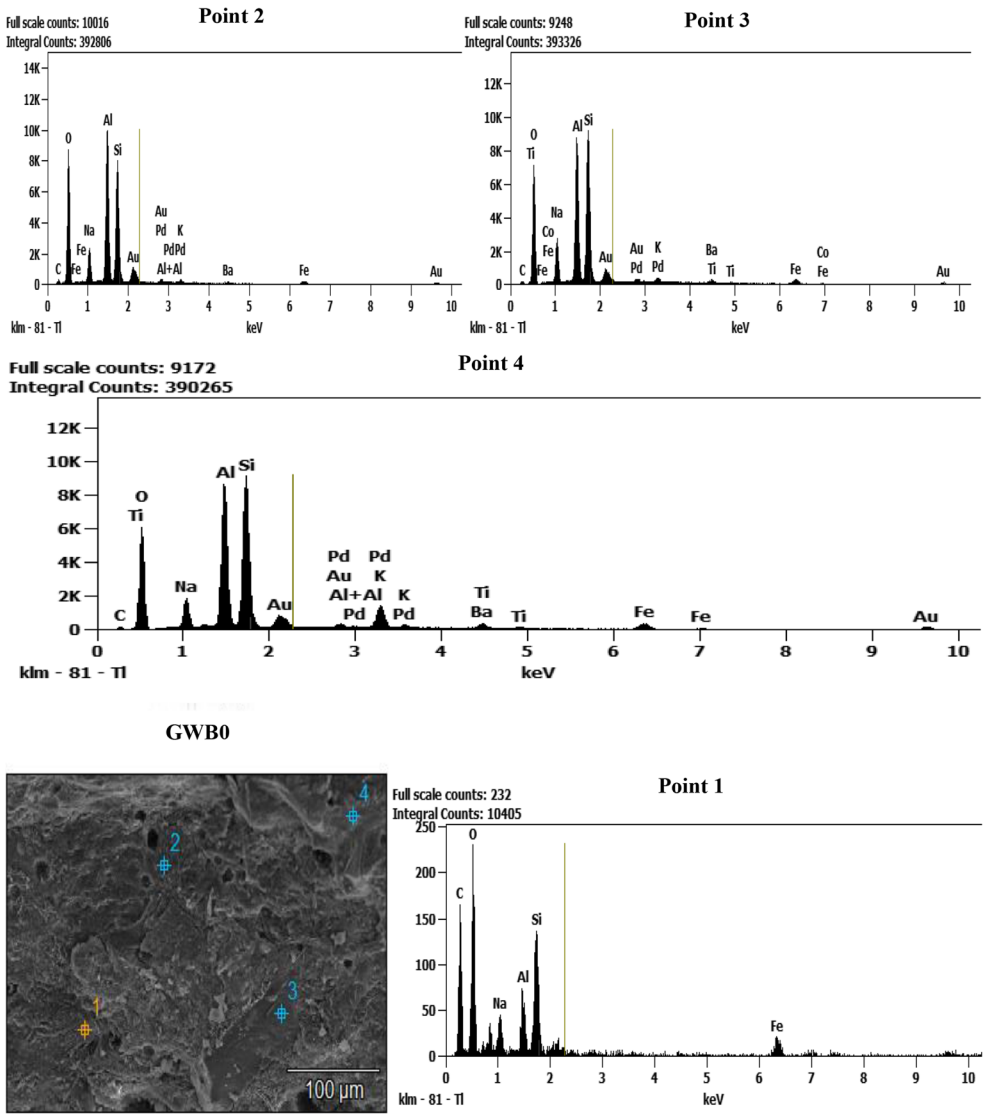

Fig. 11 (continued)

3426 cm^{-1} are recorded to the bending and stretching vibration modes of H-O-H and -OH bonds of water molecules, respectively. Those with the lowest intensity that appear at 3618 and 3686 cm^{-1} on the spectra of GWB0 and GWB100 are assigned to the residual kaolinite.

3.2.3 Micrography Images and Energy-dispersive X-ray Investigations

The micrography images of the selected geopolymer materials (GMK0, GMK75, GMK100, GWB0 and GWB100) are illustrated in Fig. 10. It can be observed that the micrographs of GMK0, GMK75, GMK100 and GWB0 are compacts and they have a homogeneous structure. The homogeneous structure of GMK0, GMK75 and GMK100 could be ascribed to the particles of quartz embedded in the matrix and therefore act as filler. Whereas the homogeneous one of GWB0 could be related to the formation of a higher siloxane chain content in the network due to the presence of the higher amorphous silica content as emphasized by the FTIR and XRD investigations. Similar observations were noted by Tchakouté et al. [32] and Zidi et al. [28]. However, when the mass ratio calcined bauxite/waste fired brick is 0.4, the fibres appear in the structure of the final product. The appearance of the fibres in GWB100 (Fig. 10) could be due to the agglomeration of the excess semi-crystalline alumina content.

The spectra of the energy dispersive X-ray analysis (EDS) of the selected geopolymer materials known as microanalysis are collected at different zones on the micrograph images at different scales (Fig. 11). It is important to note that the position of the peaks observed on each spectrum indicates the element and the intensity of each signal belongs to the

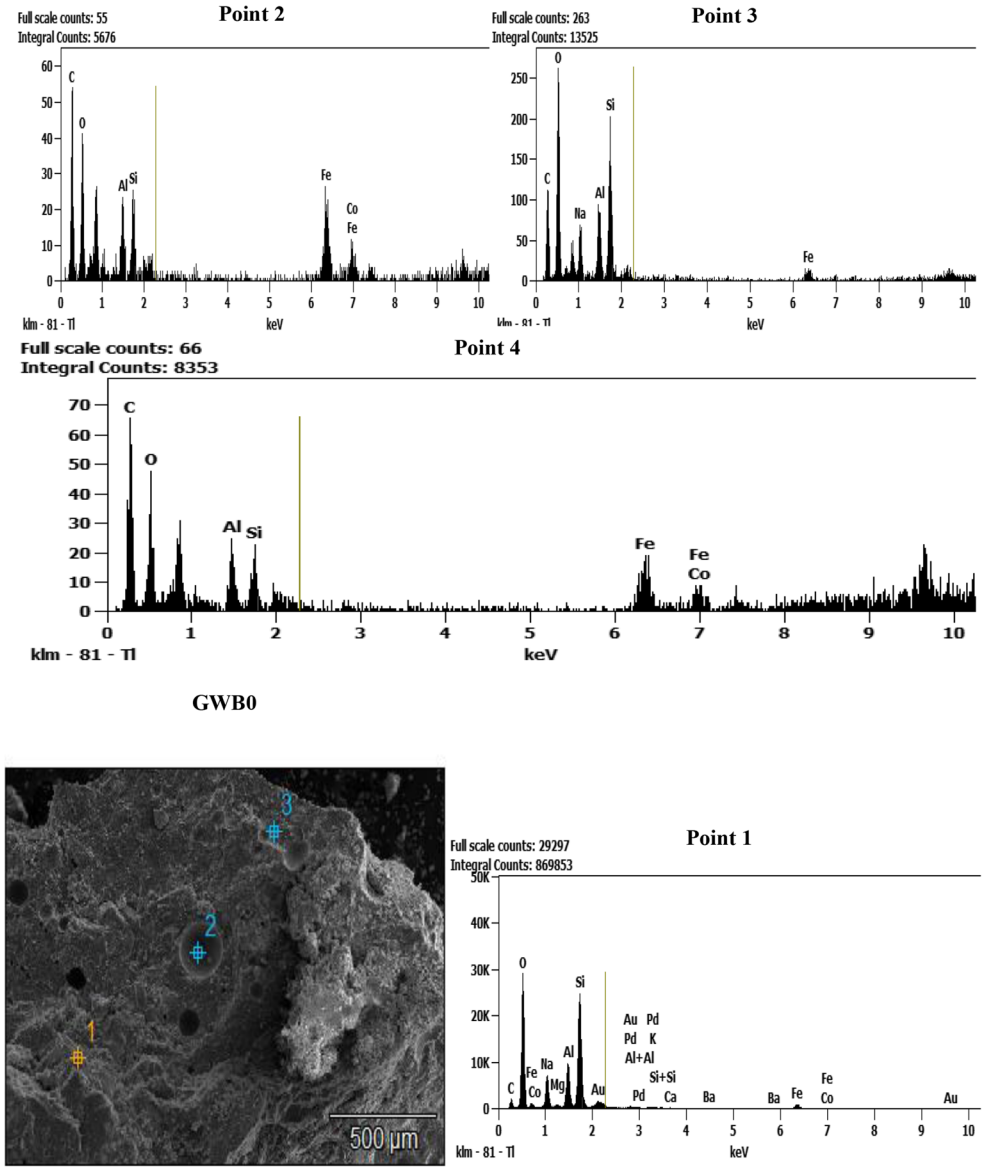

Fig. 11 (continued)

concentration of each element. The image of GMK0 observed at 200 µm presents 4 points denoted 1, 2, 3 and 4. Whereas the one at 20 µm displays 3 points (1 to 3). The spectra of the first image (1, 2, 3 and 4) indicate that the geopolymer networks are rich in silica and the image observed at 20 µm presents the same trend associated with quartz (point 1) embedded in the geopolymer matrix. The spectra of GMK75 depicts 4 points (1 to 4). Points 1 and 3 are geopolymer matrices containing some grains of quartz (points 2 and 4) but point 3 contains a higher aluminum content due to the semi-crystalline alumina added to the metakaolin during the preparation of geopolymer materials. The spectra of GMK75 show that the semi-crystalline alumina reacts with amorphous silica contained in the structure of metakaolin during the synthesis of geopolymer materials and therefore spreads in the networks. GMK75 is composed of a Si-rich geopolymer network associated with quartz embedded in the matrix. The absence of the zone rich in the alumina could be related to the fact that alumina added could be included in the network of geopolymer materials forming more sialate bonds in the system [28]. The images of GMK100 observed at 10, 25 and 100 µm present also different points. They indicate some spectra containing geopolymer networks (10 µm: point 1, 25 µm: point 2 and 100 µm: point 1) associated with Al-rich geopolymer network (10 µm: points 2, 3 and 4). The Al-rich geopolymer materials have been observed at 25 µm on points 1 and 3 and 100 µm on points 2, 3 and 4. This confirms the heterogeneity of GMK100 and the agglomeration of the excess semi-crystalline alumina in its structure. The spectra of GWB0 show the images with the scales equal to 100 µm (points 1, 2 and 3) and 500 µm

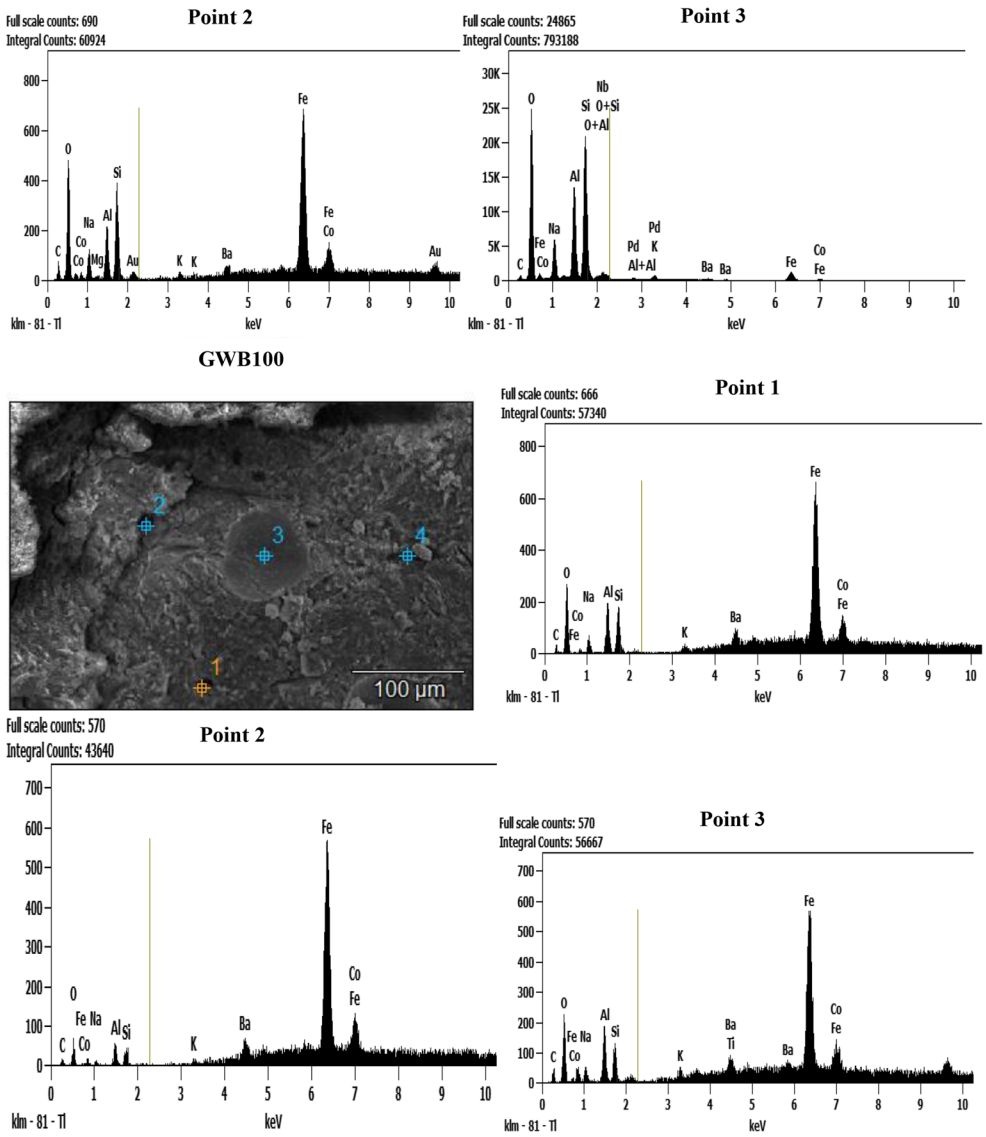

Fig. 11 (continued)

(points 1, 2, 3 and 4). These spectra indicate the formation of Si-rich geopolymer materials containing iron which spread in their structures. The EDS spectra of GWB100 reported in Fig. 11 show that the final products are mainly constituted of Al-rich geopolymer materials associated with iron due to the presence of hematite. It is as if the addition of semi-crystalline alumina to the waste fired brick in the presence of sodium waterglass would result in an agglomeration of iron hydroxide on one side and the aluminate on the other. This prevents these entities to include in the geopolymer network during the polycondensation reaction and therefore could affect negatively the compressive strength values. The image of GWB100 observed at 25 µm indicates the higher intensity of the peak of Na probably due to the lower dissolution of the raw material (waste fired brick-calcined bauxite). This is confirmed by the higher intensity of the absorption band that appears at 1388 cm^{-1} on the infrared spectrum of GWB100 (Fig. 9) compared to the one of GWB0. The higher intensity of the peak of Al observed on point 5 (GWB100) could confirm the formation of Al-OH that appears on the spectrum of GWB100 at 918 cm^{-1} (Fig. 9). It seems that the iron in the structure of GWB0 spread in the network while it is gathered in the structure of GWB100 when the semi-crystalline alumina was added to the waste fired brick. According to the EDS results of GWB100, the fibres observed on the micrograph images of GWB100 are assigned to the agglomeration of iron oxide.

3.2.4 Compressive Strengths

The compressive strength values of the geopolymer materials, GMK0, GMK25, GMK50, GMK75 and GMK100 using the

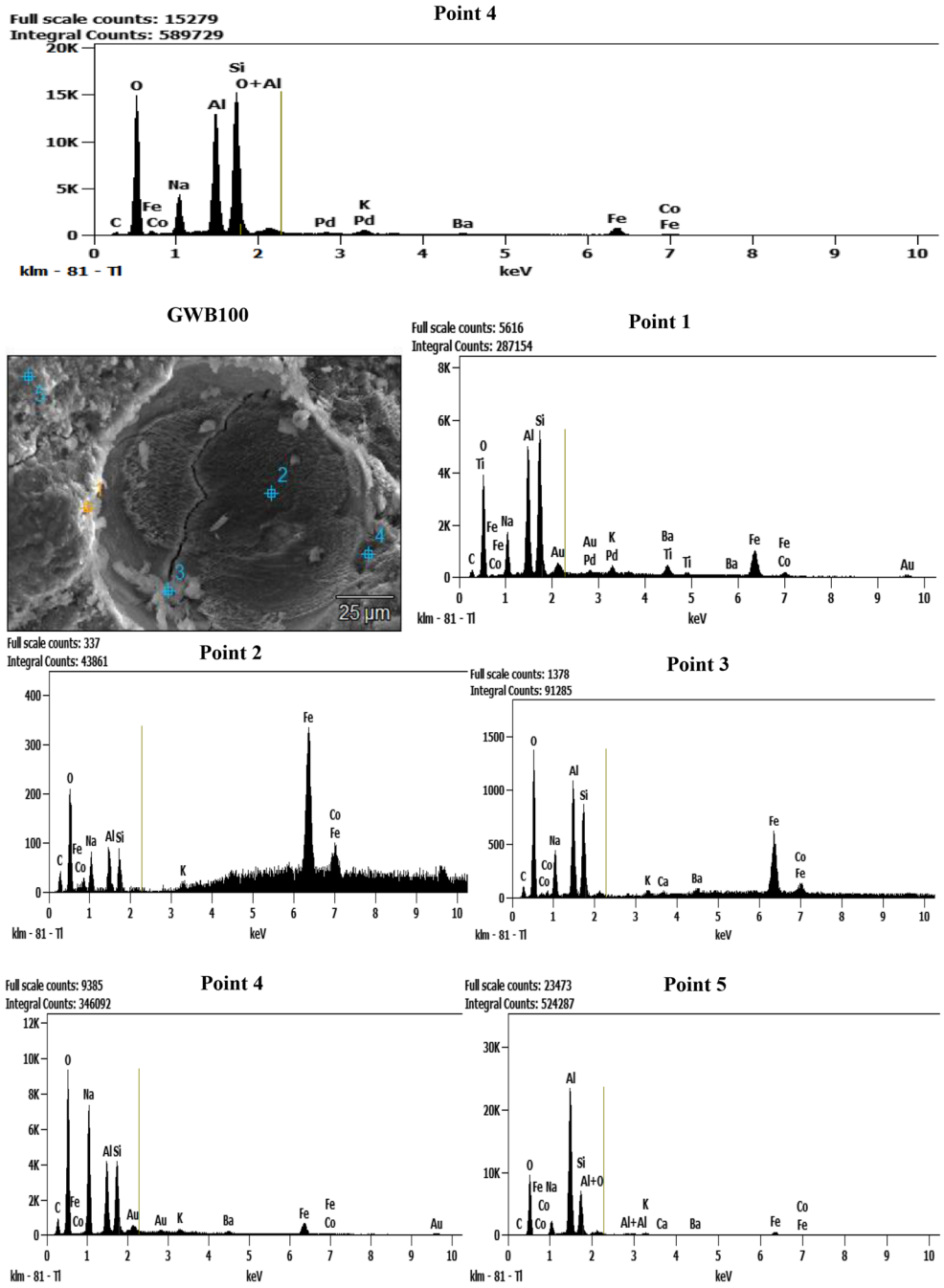

Fig. 11 (continued)

mass ratios calcined bauxite/metakaolin equals to 0, 0.1, 0.2, 0.3 and 0.4, respectively, are displayed in Fig. 12 and those of GWB0, GWB25, GWB50, GWB75 and GWB100 using calcined bauxite/waste fired brick are presented in Fig. 13. These figures show that the compressive strength values of geopolymer materials GMK0, GMK25, GMK50, GMK75 and GMK100 are 36.33, 48.44, 53.17, 55.09 and 43.19 MPa, respectively. Those of GWB0, GWB25, GWB50, GWB75 and GWB100 are 47.81, 34.94, 24.69, 23.77 and 19.91 MPa, respectively. It can be seen that the compressive strength values of the geopolymer materials from metakaolin increase from 36.33 to 55.09 MPa with the increment in the mass ratios calcined bauxite/metakaolin up to 0.3 and drop from 55.09 to 43.19 MPa when the molar ratio increases from 0.3 to 0.4. This could be ascribed to the fact that the aluminum atoms added in the system are replaced silicon atoms in Si-O-Si in metakaolin during the geopolymerization process leading to the formation of more sialate chains in the

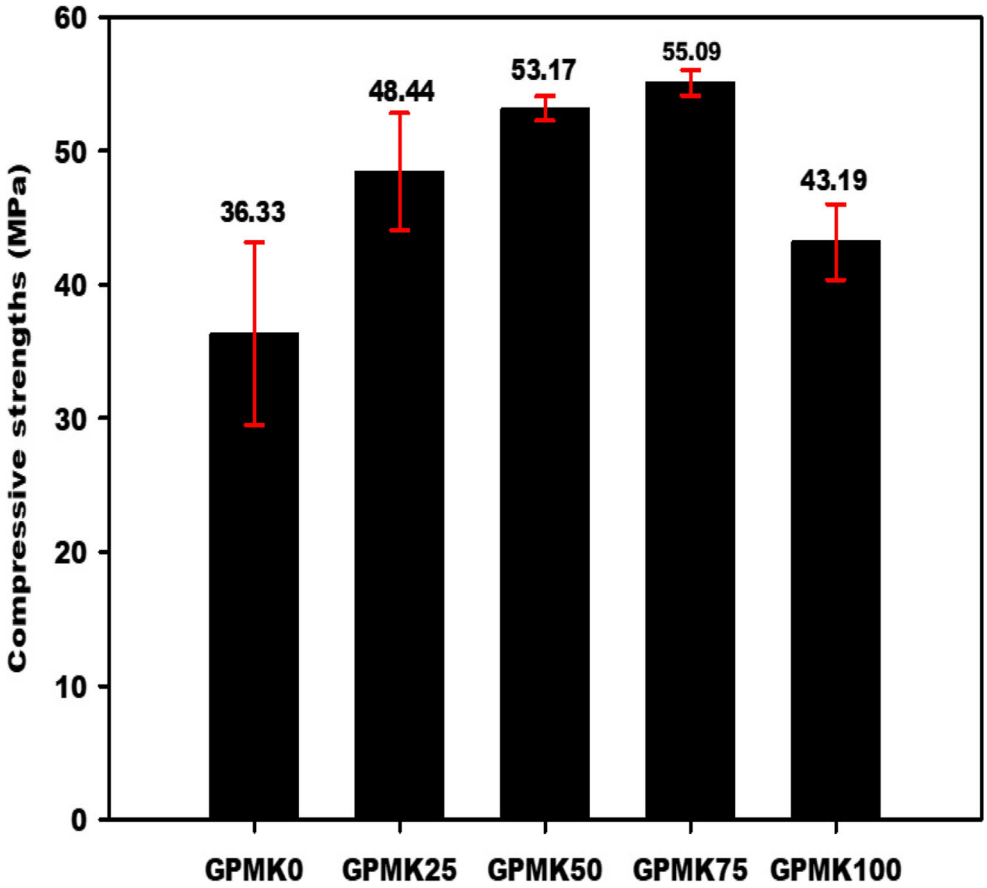

Fig. 12 Compressive strengths of geopolymer materials from mass ratios calcined bauxite/metakaolin equals to 0, 0.1, 0.2, 0.3 and 0.4

network [27]. The inclusion of more aluminum in the structure of geopolymer materials from metakaolin is justified by the lower wavenumber value of the main band which appears at about 1011 cm^{-1} compared to those from waste fired brick which appears at 1015 cm^{-1} (Figs. 8 and 9). According to Milkev [38] and Rüscher et al. [39], the inclusion of aluminum in the structure of geopolymer materials from metakaolin compared to those from waste fired brick could be related to the higher dissolution of metakaolin and therefore leading to the formation of more cross-linking geopolymer networks. The increase of the compressive strengths from 36.33 to 55.09 MPa of the geopolymer materials from metakaolin could also be assigned to the regular distribution of semi-crystalline alumina in their networks during the polycondensation process. The decrease of the strength of geopolymer materials from metakaolin could be related to the formation of Al-rich geopolymer in some zones. The obtained results are in agreement with the findings work of Fernandez-Jimenez et al. [40], De Silva et al. [41] and Fletcher et al. [42]. These authors reported that the compressive strength of the Al-rich geopolymer material is lower. This result is also confirmed by the EDS results which present some spectra with higher intensity of Al (image 10 μm, points 2 and 4). Even though the compressive strengths of geopolymer materials from metakaolin decrease from 55.09 to 43.19 MPa, the one containing the highest amount of semi-crystalline alumina (i.e. with molar ratio 0.4) is higher compared to the one prepared without the addition of semi-crystalline alumina. This could be ascribed to the inclusion of some semi-crystalline alumina in the network of GMK100 and also be related to the higher amorphous phase content in GMK100 (44 wt%) compared to the one of GMK0 which has 36 wt% of amorphous phase content (Table 4). The higher compressive strength value of GWB0 (47.81 MPa) regarding the one of GMK0 (36.33 MPa) could be related to the higher amorphous silica in the waste fired brick compared to the one of metakaolin. This amorphous silica contributes to increasing the siloxane chains in the structure of geopolymer material and therefore increase its compressive strength value [40]. This could be also be ascribed to the presence of Fe^{3+} in the structure of waste fired brick which creates more nucleation sites. Whereas, the compressive strengths of geopolymer materials from waste fired brick decrease from 47.81 to 19.91 MPa with increasing the mass ratios of calcined bauxite/waste fired brick. The decreasing of the compressive strength values of the geopolymer materials when semi-crystalline alumina was added to the waste fired brick could indicate that the semi-crystalline alumina added does not react with amorphous silica contained in the waste fired brick during the geopolymerization process. It appears that during the

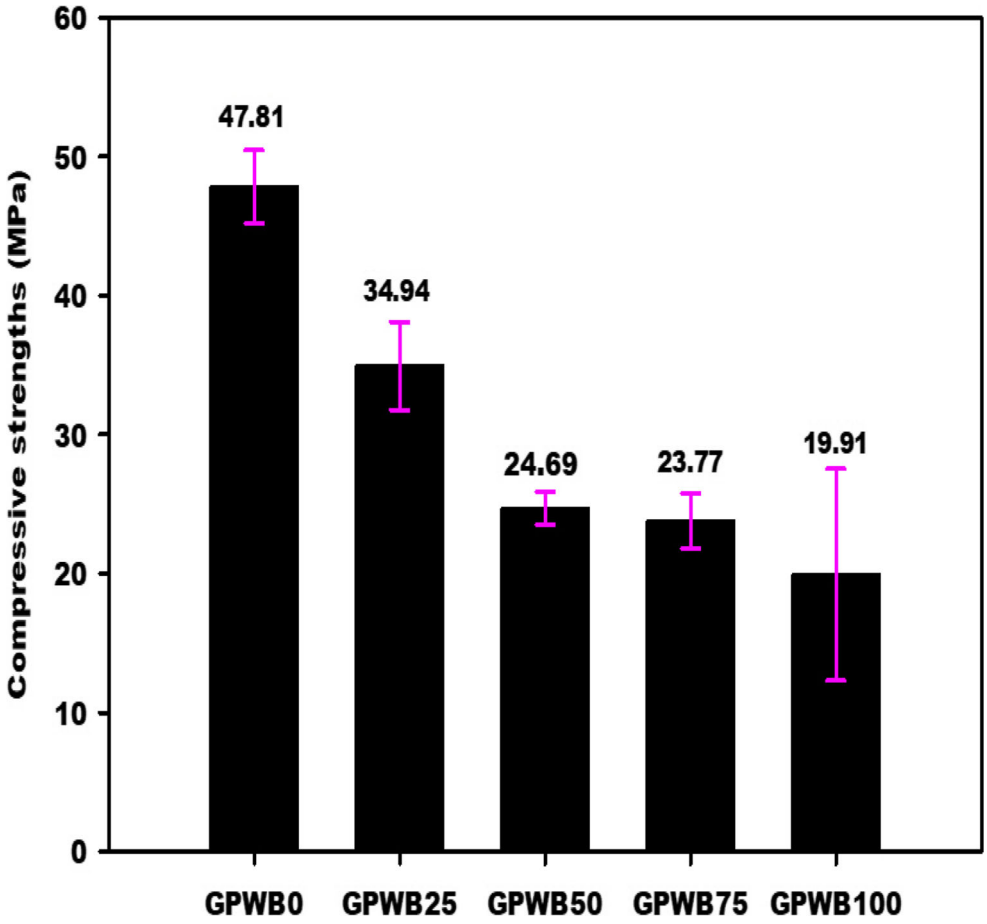

Fig. 13 Compressive strengths of geopolymers from mass ratios calcined bauxite/waste fired brick equals to 0, 0.1, 0.2, 0.3 and 0.4

geopolymerization process from waste fired brick, the additional sialate bonds do not form and therefore, aluminum from semi-crystalline alumina do not include in the network. The lowest compressive strength of GWB100 is justified by the presence of Al-OH bonds in the network. This is due to the lower dissolution of waste fired brick when semi-crystalline alumina was added entailing the formation of octahedral Al at very high Al content [43] that cannot be incorporated into the gel network.

4 Conclusions

The main objective of this investigation was to study the behavior of the semi-crystalline alumina when it is added to the aluminosilicate sources rich in quartz and amorphous silica during the synthesis of the geopolymer materials. Based on the experimental results reported, the following conclusions are drawn:

- The combination results of the chemical composition and the infrared spectra indicate that metakaolin and waste fired brick are aluminosilicate-rich in quartz and amorphous silica, respectively.
- The geopolymer materials from the mass ratios calcined bauxite/metakaolin equals 0, 0.3 and 0.4 have 36, 41.6 and 44 wt% of amorphous phases and 50, 57 and 37 wt% of quartz content, respectively. Those from the mass ratios calcined bauxite/waste fired brick equals 0 and 0.4 have 41 and 46 wt% of amorphous phases and 31 and 32 wt% of quartz content, respectively.
- The compressive strength values of the geopolymer materials from the mass ratios calcined bauxite/metakaolin equals 0, 0.1, 0.2, 0.3 and 0.4 are 36.33, 48.44, 53.17, 55.09 and 43.19 MPa, respectively. Those from calcined bauxite/waste fired brick are 47.81, 34.94, 24.69, 23.77 and 19.91 MPa, respectively.
- The micrograph images of the geopolymer materials are compact and homogeneous structures.
- The spectra of the energy dispersive X-ray analysis of geopolymer materials from metakaolin with different mass ratios calcined bauxite/metakaolin and the one from waste fired brick without adding the semi-crystalline alumina indicate the formation of Si-rich geopolymer networks. The one from waste fired brick after addition of

the semi-crystalline alumina with mass ratio calcined bauxite/waste fired brick equal to 0.4 is mainly composed of Al-rich geopolymer structures associated with iron.

It can be concluded that the semi-crystalline alumina added to the metakaolin react with amorphous silica contained in the structure of metakaolin during the preparation of geopolymer materials and therefore entails the formation of additional sialate bonds in the network. Whereas this semi-crystalline alumina does not react with amorphous silica contained in the waste fired brick during the geopolymerization entailing the agglomeration of aluminum which lead to the formation of more Al-rich geopolymer zones.

Acknowledgements Pr. Hervé Tchakouté Kouamo gratefully acknowledges Alexander von Humboldt-Stiftung for financial support for this work under the grant N° KAM/1155741 GFHERMES-P.

Author Contributions Hervé K. Tchakouté: Conceptualization, Formal analysis, Funding acquisition, Investigation, Methodology, Resources, Writing-original draft, Writing-review and editing.

Hamed I. Riyap: Methodology, Formal analysis, data curation.

B.K. Ngongang: Methodology, Data curation.

C.P.N. Nanseu: Formal analysis, Investigation, Data curation.

Claus H. Rüscher: Project administration, Formal analysis, Resources, Supervision, Validation, Visualization, Data curation.

Funding The characterization of samples was supported by Pr. Tchakouté Kouamo Hervé under the Alexander von Humboldt-Stiftung under the grant N° KAM/1155741 GFHERMES-P.

Data Availability All data generated or analysed during this study are included in this article.

Declarations This manuscript has not been published elsewhere in any form or language and has not been submitted to more than one journal for simultaneous consideration.

Ethics Approval Not applicable (The results of this study do not involve any human or animal).

Consent to Participate Not applicable.

Consent for Publication Not applicable.

Conflict of Interest No potential conflict of interest was reported by the authors.

Disclosure of Potential Conflicts of Interest We wish to draw the attention of the Editor to the following facts which may be considered as potential conflicts of interest and to significant financial contributions to this work. We wish to confirm that there are no known conflicts of interest associated with this publication and there has been no significant financial support for this work that could have influenced its outcome. We confirm that the manuscript has been read and approved by all named authors and that there are no other persons who satisfied the criteria for authorship but are not listed. We further confirm that the order of authors listed in the manuscript has been approved by all of us. We confirm that we have given due consideration to the protection of intellectual property associated with this work and that there are no impediments to publication, including the timing of publication, with respect to intellectual property. In so doing we confirm that we have followed the regulations of our institutions concerning intellectual property. We further confirm that any aspect of the work covered in this manuscript that has involved either experimental animals or human patients has been conducted with the ethical approval of all relevant bodies and that such approvals are acknowledged within the manuscript. We understand that the Corresponding Author is the sole contact for the Editorial process (including Editorial Manager and direct communications with the office). He/she is responsible for communicating with the other authors about progress, submissions of revisions and final approval of proofs. We confirm that we have provided a current, correct email address which is accessible by the Corresponding Author and which has been configured to accept email from htchak@yahoo.fr.

Research Involving Human Participants and/or Animals. Not applicable.

Informed Consent Not applicable.

References

1. Davidovits J (2017) Geopolymers: ceramic-like inorganic polymers. J Ceram Sci Technol 8:335–350
2. Tchakouté HK, Melele SJK, Nanseu-Njiki CP, Rüscher CH (2021) Semi-adiabatic calorimetry to determine the temperature and the time of the formation of faujasite and geopolymer gels in the composites prepared at room temperature and the investigation of the properties of the hardened composites. Silicon. https://doi.org/10.1007/s12633-021-01267-1
3. Gao K, Lin KL, Wang D, Hwang CL, Shiu HS, Chang YM, Cheng TW (2014) Effect of SiO metakaolin-based geopolymers. Constr Build Mater 53:503–510
4. Le-ping L, Xue-min C, Shu-heng Q, Jun-li Y, Lin Z (2010) Preparation of phosphoric acid-based porous geopolymers. Appl Clay Sci 50:600–603
5. Douiri H, Louati S, Baklouti S, Arous M, Fakhfakh Z (2014) Structural, thermal and dielectric properties of phosphoric acid-based geopolymers with different amounts of H_3PO_4. Mater Lett 116:9–12
6. Louati S, Hajjaji W, Baklouti S, Samet B (2014) Structure and properties of new eco-material obtained by a phosphoric acid attack of natural Tunisian clay. Appl Clay Sci 101:60–67
7. Tchakouté HK, Rüscher CH (2017) Mechanical and microstructural properties of metakaolin-based geopolymer cements from sodium waterglass and phosphoric acid solution as hardeners: A comparative study. Appl Clay Sci 140:81–87
8. Mathivet V, Jouin J, Gharzouni A, Sobrados I, Celerier H, Rossignol S, Parlier M (2019) Acid-based geopolymers: Understanding of the structural evolutions during consolidation and after thermal treatments. J Non-Cryst Solids 512:90–97
9. Bewa CN, Tchakouté HK, Fotio D, Rüscher CH, Kamseu E, Leonelli C (2018) Water resistance and thermal behaviour of metakaolin-phosphate-based geopolymer cements. J Asian Ceram Soc 6:271–283
10. Banenzoué C, Bewa CN, Fotio D, Tchakouté HK, Tchanga BT, Rüscher CH (2021) Physical properties and microstructures of poly(phospho-siloxo) and poly(sialate-siloxo) networks from two metakaolins. J Korean Ceram Soc 58:452–470
11. Riyap HI, Tazune FK, Fotio D, Tchakouté HK, Nanseu-Njiki CP, Rüscher CH (2021) The coexistence of the poly(phospho-siloxo)

networks and calcium phosphates on the compressive strengths of the acid-based geopolymers obtained at room temperature. J Inorg Organomet Polym Mater 31:3301–3323
12. Davidovits J (2011) Geopolymer Chemistry and Applications, 3rd edn. Institute Geopolymer, Saint-Quentin, p 612
13. Bewa CN, Tchakouté HK, Banenzoué C, Cakanou L, Mbakop TT, Kamseu E, Rüscher CH (2020) Acid-based geopolymers using waste fired brick and different metakaolins as raw materials. Appl Clay Sci 198:105813
14. Elimbi A, Tchakoute HK, Njopwouo D (2011) Effects of calcination temperature of kaolinite clays on the properties of geopolymers cements. Constr Build Mater 25:2805–2812
15. Kaze RC, Beleuk à Moungam LM, Djouka MLF, Nana A, Kamseu E, Melo UFC (2017) The corrosion of kaolinite by iron minerals and the effects on geopolymerization. Appl Clay Sci 138:48–62
16. Nkoumbou C, Njoya A, Njoya D, Grosbois C, Njowouo D, Yvon J, Martin F (2009) Kaolin from Mayouom (Western Cameroon): industrial suitability evaluation. Appl Clay Sci 43:118–124
17. Lemougna PN, Melo UFC, Kamseu E, Tchamba AB (2011) Laterite based stabilized products for sustainable building applications in tropical countries: review and prospects for the case of Cameroon. Sustainability 3:293–305
18. Lemougna PN, Mackenzie KJD, Melo UFC (2011) Synthesis and thermal properties of inorganic polymers (geopolymers) for structural and refractory applications from volcanic ash. Ceram Int 37: 3011–3018
19. Tchakouté HK, Elimbi A, Yanne E, Djangang CN (2013) Utilization of volcanic ashes for the production of geopolymers cured at ambient temperature. Cem Concr Compos 38:75–81
20. Siddique R, Khan MI (2011) Supplementary cementing materials. Springer Science & Business 716 Media
21. Tchakouté HK, Rüscher CH, Kong S, Ranjbar N (2016) Synthesis of sodium waterglass from white rice husk ash as an activator to produce metakaolin-based geopolymer cements. J Build Eng 6: 252–261
22. Tchakouté HK, Rüscher CH, Hinsch M, Djobo JNY, Kamseu E, Leonelli C (2017) Utilization of sodium waterglass from sugar cane bagasse ash as a new alternative hardener for producing metakaolin-based geopolymer cement. Geochem 77:257–266
23. Shaikh IR, Shaikh AB (2013) Utilization of wheat husk ash as silica source for the synthesis of MCM-41 type mesoporous silicates: a sustainable approach towards valorization of the agricultural waste stream. Res J Chem Sci 3:66–72
24. Nguimatsia DFW, Yongue FR (2015) Geological contribution to the Fongo Tongo bauxite formations (west-Cameroon). J Geol Geosci 4:3. International Conference on Geology, June 22–23, Florida, USA
25. Tchamba AB, Yongue R, Melo UC, Kamseu E, Njoya D, Njopwouo D (2008) Caractérisation de la bauxite de Haléo-Danielle (Minim-Martap, Cameroun) en vue de son utilisation industrielle dans les matériaux à haute teneur en alumine. Silic Ind 73:77–83
26. Lima MSS, Thives LP, Haritonovs V, Bajars K (2017) Red mud application in construction industry: review of benefits and possibilities. IOP Conf Ser: Mater Sci Eng 251:012033
27. Le VQ, Do QM, Hoang MD, Nguyen HT (2018) The role of active silica and alumina in geopolymerization. Vietnam J Sci Technol Eng 60:16–23
28. Zidi Z, Ltifi M, Ben Ayadi Z, El Mir L (2019) Synthesis of nano-alumina and their effect on structure, mechanical and thermal properties of geopolymer. J Asian Ceram Soc 7:524–535
29. Phoo-ngernkham T, Chindaprasirt P, Sata V, Hanjtsuwan S, Hatanaka S (2014) The effect of adding nano-SiO_2 and nano-Al_2O_3 on properties of high calcium fly ash geopolymer cured at ambient temperature. Mater Des 55:58–65
30. Zheng L, Wang W, Shi YC (2010) The effects of alkaline dosage and Si/Al ratio on the immobilization of heavy metals in municipal solid waste incineration fly ash-based geopolymer. Chemosphere 79:665–671
31. Duxson P, Provis JL, Lukey GC, Mallicaot SW, Kriven WK, van Deventer JSJ (2005) Understanding the relationship between geopolymer composition, microstructure and mechanical properties. Colloid Surf A: Physicochem Eng Aspects 269:47–58
32. Tchakouté HK, Elimbi A, Mbey JA, Sabouang CJN, Njopwouo D (2012) The effect of adding alumina-oxide to metakaolin and volcanic ash on geopolymer products: A comparative study. Constr Build Mater 35:960–969
33. Melele SJK, Banenzoué C, Fotio D, Tchakouté HK, Rüscher CH, Nanseu CPN (2019) Improvement of the reactivity of soda-lime–silica glass solution as a hardener for producing geopolymer materials. SN Appl Sci 1:1–16
34. Beleuk à Moungam LM, Mohamed H, Kamseu E, Billong N, Melo UFC (2017) Properties of geopolymers made from fired clay bricks wastes and rice husk ash (RHA)-sodium hydroxide (NaOH) activator. Mater Sci Appl 8:537–552
35. Moudio AMN, Tchakouté HK, Ngnintedem DLV, Andreola F, Kamseu E, Nanseu-Njiki CP, Leonelli C, Rüscher CH (2021) Influence of the synthetic calcium aluminate hydrate and the mixture of calcium aluminate and silicate hydrates on the compressive strengths and the microstructure of metakaolin-based geopolymer cements. Mater Chem Phys 264:124459
36. Tironi A, Trezza MA, Scian AN, Irassar EF (2012) Kaolinitic calcined clays: factors affecting its performance as pozzolans. Constr Build Mater 28:276–281
37. Tchakouté HK, Rüscher CH, Djobo JNY, Kenne BBD, Njopwouo D (2015) Influence of gibbsite and quartz in kaolin on the properties of metakaolin-based geopolymer cements. Appl Clay Sci 107:188–194
38. Milkey RG (1960) Infrared spectra of some tectosilicates. Am Mineral 45:990–1007
39. Rüscher CH, Mielcarek E, Lutz W, Ritzmann A, Kriven WM (2010) Weakening of alkali-activated metakaolin during aging investigated by the molybdate method and infrared absorption spectroscopy. J Am Ceram Soc 93:2585–2590
40. Fernández-Jiménez A, Palomo A, Sobrados I, Sanz J (2018) The role played by the reactive alumina content in the alkaline activation of fly ashes. Microporous Mesoporous Mater 91:111–119
41. De Silva P, Sagoe-Crenstil K, Sirivivatnanon V (2007) Kinetics of geopolymerization: role of Al_2O_3 and SiO_2 Cem Concr Res 37: 512–518
42. Fletcher RA, Mackenzie KJD, Nicholson CL, Shimada S (2005) The composition range of aluminosilicate geopolymers. J Eur Ceram Soc 25:1471–1477
43. Wittf BM, Uytterhoeven JB (1996) Acid and alkaline sol–gel synthesis of amorphous aluminosilicates, dry gel properties, and their use in probing sol phase reactions. J Colloid Interface Sci 181:200–207